Received: 16 June 2020 | Revised: 14 October 2020 | Accepted: 15 October 2020

DOI: 10.1002/cne.25058

RESEARCH ARTICLE

JCN RESEARCH IN SYSTEMS NEUROSCIENCE THE JOURNAL OF COMPARATIVE NEUROLOGY WILEY

Distribution of the cholinergic nuclei in the brain of the weakly electric fish, *Apteronotus leptorhynchus*: Implications for sensory processing

Brenda Toscano-Márquez[1] | Livio Oboti[2] | Erik Harvey-Girard[3] | Leonard Maler[3] | Rüdiger Krahe[1,2]

[1]Department of Biology, McGill University, Montreal, Quebec, Canada

[2]Humboldt-Universität zu Berlin, Institut für Biologie, Berlin, Germany

[3]Department of Cellular and Molecular Medicine, University of Ottawa, Ottawa, Ontario, Canada

Correspondence
Rüdiger Krahe and Livio Oboti, Institut für Biologie, Humboldt-Universität zu Berlin, 10099 Berlin, Germany.
Email: ruediger.krahe@hu-berlin.de (R. K.) and livio.oboti@hu-berlin.de (L. O.)

Funding information
Canada Foundation for Innovation, Grant/Award Number: 9604; Canadian Institutes of Health Research, Grant/Award Number: 6027; Canadian Network for Research and Innovation in Machining Technology, Natural Sciences and Engineering Research Council of Canada, Grant/Award Numbers: 04336, 2009-293306, 2014-05364; Deutsche Forschungsgemeinschaft, Grant/Award Number: EXC257/2; Le Fonds Québécois de la Recherche sur la Nature et les Technologies, Grant/Award Number: 2012 PR-145726; Merit Scholarship for Foreign Students

Abstract

Acetylcholine acts as a neurotransmitter/neuromodulator of many central nervous system processes such as learning and memory, attention, motor control, and sensory processing. The present study describes the spatial distribution of cholinergic neurons throughout the brain of the weakly electric fish, *Apteronotus leptorhynchus*, using in situ hybridization of choline acetyltransferase mRNA. Distinct groups of cholinergic cells were observed in the telencephalon, diencephalon, mesencephalon, and hindbrain. These included cholinergic cell groups typically identified in other vertebrate brains, for example, motor neurons. Using both in vitro and ex vivo neuronal tracing methods, we identified two new cholinergic connections leading to novel hypotheses on their functional significance. Projections to the nucleus praeeminentialis (nP) arise from isthmic nuclei, possibly including the nucleus lateralis valvulae (nLV) and the isthmic nucleus (nI). The nP is a central component of all electrosensory feedback pathways to the electrosensory lateral line lobe (ELL). We have previously shown that some neurons in nP, TS, and tectum express muscarinic receptors. We hypothesize

Abbreviations: cELL, commissure of the electrosensory lateral line lobe; CC, crista cerebellaris; CCb, corpus cerebelli; CLS, centrolateral segment of the ELL; CMS, centromedial segment of the ELL; DD, dorsodorsal telencephalon; DFI, lateral subdivision of the diffuse nucleus of the inferior lobe; DL, dorsolateral telencephalon; DLv, dorsolateral telencephalon ventral subdivision; DM2v/d, dorsomedial division of the telencephalon (dorsal and ventral); Dp, dorsal posterior telencephalon; DPl, lateral subdivision of the caudal DP; DPm, medial subdivision of the caudal DP; EGp, eminentia granularis pars posterior; ELL, electrosensory lateral line lobe; Er, rostral entopeduncular nucleus; Ha, anterior hypothalamic nucleus; IXm, glossopharyngeal nucleus; LFB, lateral forebrain bundle; LL, lateral lemniscus; LR, lateral reticular nucleus; LVII, facial lobule; MLF, medial longitudinal fasciculus; MOTf, medial olfactory terminal field; MRF, mesencephalic reticular formation; MS, medial segment of the ELL; nAPV, nucleus anterior periventricularis; nE, nucleus electrosensorius; nI, nucleus isthmi; nIII, oculomotor nucleus; nIV, trochlear nucleus; nIXm, glossopharyngeal nucleus; nLV, nucleus lateralis valvulae; nM, nucleus medialis; nP, nucleus praeeminentialis; nVm, trigeminal motor nucleus; nXm, vagal motor nucleus; nXs, vagal sensory nucleus; OE, octavolateral efferent nucleus; PG, preglomerular nucleus; PGr, rostral part of the preglomerular nucleus; PLm, medial subdivision of the paralemniscal nucleus; PRF, paramedian reticular formation; POC, postoptic commissure; PPp, posterior subdivision of the preoptic nucleus; PT, pretectal nucleus; Rd, nucleus raphe dorsalis; RF, reticular formation; Sc, suprachiasmatic nucleus; SG/V, secondary gustatory/visceral nucleus; smc, spinal motor column; SPV, stratum periventriculare; SRn, superior reticular nucleus; ST, subtoral nucleus; STr, subtrigeminal nucleus; TA, nucleus tuberis anterior; TeO, optic tectum; tLT, lateral trigeminal tract; TS, torus semicircularis; TSd, torus semicircularis dorsalis; tStF, tractus stratum fibrosum; tSP-Cb, spino-cerebellar tract; tVd, descending trigeminal tract; v, ventricle; Vc, central division of ventral telencephalon; VCb, valvula cerebelli; Vd, dorsal subdivision of the ventral telencephalon; Vh, ventral horn; nVIIm, facial motor nucleus; Vl, intermediate subdivision of the ventral telencephalon; VIr, intermediate rostral subdivision of the ventral telencephalon; VP, valvular peduncle; Vp, posterior subdivision ventral telencephalon; Vs, supracommissural subdivision of the ventral telencephalon; VVv, ventral part of the ventral subdivision of ventral telencephalon; ZT, transitional zone.

Brenda Toscano-Márquez and Livio Oboti contributed equally to this study.

that, based on nLV/nI cell responses in other teleosts and isthmic connectivity in *A. leptorhynchus*, the isthmic connections to nP, TS, and tectum modulate responses to electrosensory and/or visual motion and, in particular, to looming/receding stimuli. In addition, we found that the octavolateral efferent (OE) nucleus is the likely source of cholinergic fibers innervating the ELL. In other teleosts, OE inhibits octavolateral hair cells during locomotion. In gymnotiform fish, OE may also act on the first central processing stage and, we hypothesize, implement corollary discharge modulation of electrosensory processing during locomotion.

KEYWORDS

acetylcholine, electrosensory system, gymnotiform, neuromodulation, tract tracing, weakly electric fish

1 | INTRODUCTION

Acetylcholine (ACh) can act as a neurotransmitter at the neuromuscular junction and in the autonomic nervous system, whereas it acts both as a neurotransmitter and as a neuromodulator in the central nervous system (see Picciotto et al., 2012, for review). ACh is present in the nervous systems of invertebrates as well as vertebrates including mammals and it has attracted attention because it plays a pivotal role in fundamental brain processes from motor control to higher cognitive function (Hasselmo, 2006; Mooney et al., 2004; Sarter et al., 2005; Woolf & Butcher, 2011). ACh has also been shown to be a widespread modulator of information transmission in sensory systems (Fournier et al., 2004; Mooney et al., 2004; Woolf & Butcher, 2011). It controls receptive field properties and the gain of sensory responses, can enhance the signal-to-noise ratio of visual and auditory activity (Kimura, 2000; Sato et al., 1987; Sillito et al., 1983; Sillito & Kemp, 1983), and is involved in gustatory (Baldo et al., 2013; Hasegawa & Ogawa, 2007) and olfactory (Chan et al., 2017; de Almeida et al., 2016; Smith et al., 2015) processing. Importantly, the ACh projections from nucleus isthmi (nI) to tectum play a critical role in stimulus selection when multiple potential visual or auditory targets are present (Asadollahi et al., 2011; Maczko et al., 2006; Schmidt, 1995).

Choline acetyltransferase (ChAT) is the enzyme responsible for catalyzing the transfer of an acetyl group from acetyl-coenzyme A to choline, the step that forms ACh. As ChAT is exclusively expressed in ACh-synthesizing neurons, it has been used as a specific marker for studying the distribution and development of cholinergic neurons (see Oda, 1999, for review). The distribution of ChAT-containing cells has been described in several organisms from invertebrates to fish and mammals, including rats and humans (reviewed in Clemente et al., 2005; Ichikawa et al., 1997; Kasashima et al., 1998; Yasuyama & Salvaterra, 1999). These studies have contributed to the characterization of common organization and distribution of cholinergic neurons allowing the identification of homologous cell groups across taxa. Despite strong overall agreement between distribution patterns, some species-specific variations have been found (Anadón et al., 2000; Clemente et al., 2005; López et al., 2013; Morona et al., 2013).

The electrosensory system of brown ghost knifefish, *Apteronotus leptorhynchus*, has proven to be a fruitful model to study sensory processing (e.g., Chacron et al., 2011; Clarke et al., 2015; Clarke & Maler, 2017; Krahe & Maler, 2014; Toscano-Márquez, Krahe, & Chacron, 2013), behavior (e.g., Dunlap et al., 2013; Silva et al., 2013; Walz et al., 2013), as well as learning and memory (e.g., Harvey-Girard et al., 2010; Jun et al., 2016). Much of the brain circuitry of gymnotiform weakly electric fish is dedicated to processing electrosensory information streaming in from electroreceptor organs distributed over the skin of the animals (Bell & Maler, 2005). The electroreceptors respond to perturbations of a weak, self-generated, electric field. These perturbations can be caused by objects in the environment (electrolocation) or the electric fields of other weakly electric fish (electrocommunication). Modulation of the response properties of central electrosensory neurons by ACh has already been documented in *A. leptorhynchus* (Ellis et al., 2007; Toscano-Márquez, Dunn, & Krahe, 2013; Toscano-Márquez, Krahe, & Chacron, 2013). Application of the cholinergic agonist carbachol led to increased excitability, burst firing, and shifts in frequency tuning of pyramidal cells in the first-order central processing stage of electrosensory inputs, the electrosensory lateral line lobe (ELL) of the hindbrain. These effects could be occluded by prior application of the muscarinic receptor antagonist atropine (Ellis et al., 2007). In a previous study, we mapped the distribution of muscarinic receptors in the brain of *A. leptorhynchus* (Toscano-Márquez, Dunn, & Krahe, 2013). We identified three subtypes of muscarinic receptors, whose distribution suggests that ACh likely modulates electrosensory information processing at stages from at least hindbrain (ELL) to midbrain and diencephalon, and also affects other sensory modalities and higher brain processes (Toscano-Márquez, Dunn, & Krahe, 2013).

The goal of the present study was to identify the sources of ACh in the brain of *A. leptorhynchus*, with a focus on the sources of ACh released in electrosensory areas. We mapped the distribution of ChAT messenger RNA and used retrograde labeling to identify cholinergic cell groups projecting to electrosensory nuclei previously shown to

express muscarinic receptors (Toscano-Márquez, Dunn, & Krahe, 2013).

2 | METHODS

2.1 | Animals

We used weakly electric fish, *A. leptorhynchus*, of both sexes for this study (n = 20). The animals were obtained from a local supplier and maintained on a 12 h light cycle in tanks at a temperature of 26–28°C. All procedures were approved by the animal care committees of McGill University and the University of Ottawa. The ex vivo DiI tracing was approved by the Landesamt für Gesundheit und Soziales of Berlin, Germany (# T 0087/19).

As initial attempts to use commercial antibodies against ChAT failed, we decided to use an in situ hybridization approach to map the expression of ChAT-positive cell bodies.

2.2 | Cloning and sequencing of ChAT mRNA

Two fish were anesthetized with 500 ppm buffered 3-aminobenzoic acid ethyl ester (MS222; Sigma, St. Louis, MO) in cold water and ice. The brains were rapidly removed and homogenized in TRI reagent solution (Ambion, Austin, TX) to obtain total RNA. cDNAs were generated using SuperScript III kit (Invitrogen, Carlsbad, CA) according to the manufacturer's instructions. The resulting cDNA was used to clone a fragment of the ChAT sequence using a forward primer (5′-GTG TCV ACC TAY GAG AGY GC-3′) and reverse primer (5′-GCR CTC TCR TAG GTB GAC AC-3′) that produced a 730 bp-long product. The ChAT sequence was isolated using a pair of primers designed to start and end the amplification in a conserved region of the ChAT sequence, based on a comparison of mouse (NM_009891.2), zebrafish (NM_001130719), fugu (ENSTRUT00000028871), and stickleback (ENSGACT00000003248) sequences taken from GenBank (Bethesda, MD) and Ensembl (www.ensembl.org).

The purified PCR product was inserted into pGEM-T vector (Promega, Madison, WI) following the manufacturer's guidelines. Plasmid DNA clones were purified using a DNA purification kit (Promega) and linearized using primers that targeted the M13 forward or reverse sites of the vector. The clones that showed a similar size to the expected ChAT sequence were sent for sequencing to the Genome Quebec Innovation Center.

Nucleotide and predicted protein sequences were analyzed using the ClustalW method in Geneious sequence alignment editor (Biomatters Ltd., Auckland, New Zealand; version 5.3). We performed a protein sequence alignment between the partial cDNA PCR fragment that we obtained for *A. leptorhynchus* and the corresponding fragments of other ChAT deduced amino acid sequences from GenBank and Ensembl. We used ChAT from *Drosophila* as outgroup. To produce the phylogenetic tree, we used the Phylogeny Inference Package (PHYLIP; Felsenstein, 1989). The aligned amino acid sequences were resampled by bootstrapping 1,000 times in the SEQBOOT program of PHYLIP. Calculations of phylogenetic distances using the maximum likelihood estimates based on the Dayhoff PAM matrix were performed in PROTDIST. The tree was determined by the UPGMA method using the NEIGHBOR program. Finally, a consensus tree was determined in CONSENSE. We used the following species (accession numbers): African clawed frog (*Xenopus laevis*; XP_033799462), American green anole (*Anolis carolinensis*; XP_003223305), Australian ghostshark (*Callorhinchus milii*; XP_007896569), channel catfish (*Ictalurus punctatus*; XP_017338290), chicken (*Gallus gallus*; XP_015143441), common carp (*Cyprinus carpio*; XP_018936692), electric eel (*Electrophorus electricus*; XM_027027579), fruit fly (*Drosophila melanogaster*; NP_477004.5), green sea turtle (*Chelonia mydas*; XP_007067297), human (*Homo sapiens*; NP_001136401.2, mouse (*Mus musculus*; AAI19323), Nile tilapia (*Oreochromis niloticus*; XP_005471447), red-bellied piranha (*Pygocentrus nattereri*; XP_017570822), peregrine falcon (*Falco peregrinus*; XP_005236805), saltwater crocodile (*Crocodylus porosus*; XP_019411902), sansaifugu (*Takifugu flavidus* TWW81966), sea lamprey (*Petromyzon marinus*; XP_032814983), Southern platyfish (*Xiphophorus maculatus*; XP_005794628.1), thorny skate (*Amblyraja radiate*; XP_032868510), whale shark (*Rhincodon typus*; XP_020381721), West Indian Ocean coelacanth (*Latimeria chalumnae*; XP_005992503), zebrafish (*Danio rerio*; NP_001124191.1).

2.3 | RNA probe preparation

The RNA probes for in situ hybridization were synthesized using digoxigenin (DIG) UTP RNA Labeling Kit Sp6/T7 (Roche Applied Science, Indianapolis, IN) according to the manufacturer's recommendations.

2.4 | Histological processing

Three fish were anesthetized with 200 ppm of buffered MS222 and perfused first with cold phosphate buffer (PBS: NaCl 140 mM, KCl 2.5 mM, KH_2PO_4 1.5 mM, Na_2HPO_4 6 mM; pH 7.4) followed by cold PBS containing 4% paraformaldehyde (4% PBS-PFA) via a 30-gauge needle inserted in the conus arteriosus. The brains were removed and placed overnight in 4% PFA-PBS solution at 4°C. After overnight fixation, the brains were cryoprotected in a PBS/30% sucrose solution overnight at 4°C. Transverse and sagittal sections of 25 μm were obtained in a cryostat and stored at −20°C until use.

2.5 | In situ hybridization

We performed in situ hybridization as described in Toscano-Márquez, Dunn, and Krahe (2013). Briefly, slides containing the brain sections were postfixed in 4% PFA-PBS buffer and rinsed in PBS (pH 7.4) for 5 min at room temperature (RT), permeabilized with 0.3% Triton X-100/PBS for 15 min at RT and, after PBS washes, digested by proteinase K (5 μg/ml) in Tris-EDTA buffer (100:50) for 30 min at 37°C

(Invitrogen, 5 ng/ml). After two rinses with PBS for 5 min at RT, they were rinsed with 0.1 M triethanolamine (TEA) buffer, pH 8.0, and incubated for 2 min at RT and acetylated with 0.25% acetic anhydride/TEA. Slides were preincubated for 1 h in a hybridization solution containing 50% formamide, 0.75 M NaCl, 25 mM PIPES, 1x Denhardt's solution, 0.2% Tween 20, 1 mg/ml salmon sperm DNA, 1 mg/ml yeast tRNA at 60°C. The slides were hybridized overnight in the hybridization solution containing the diluted RNA DIG-labeled probe and 10% dextran sulfate at 60°C. After hybridization, the slides were washed twice at the same temperature in descending sodium-citrate buffer solutions (2X SSC, 1X SSC/50% formamide, 0.2X SSC), followed by three washes in 100 mM Tris, 150 mM NaCl, pH 7.5 at RT. Slides were mounted applying coverslips (Corning, 2975245, Thermo Fisher Scientific) on a drop of mounting medium suited for either bright-field (DPX, 06522, Sigma Aldrich) or fluorescence imaging (Fluoromount, F4680, Sigma Aldrich).

The immunodetection of the hybridized DIG probes was performed as follows. The slides were incubated in blocking solution containing the Tris washing buffer with 0.1% Triton X-100, 2% normal sheep serum, 1% blocking reagent (Roche Life Science, Indianapolis, IN), followed by a 2-h incubation in a humid chamber with anti–DIG alkaline phosphatase antibody (Roche; 1:1,000 dilution) in the blocking buffer. Detection was developed using coloration solution consisting of a mix of 3% 4-nitroblue tetrazolium chloride/5-bromo 4-chloro 3-indol phosphate in Tris-$MgCl_2$ (100 mM Tris–HCl, pH 9.5) buffer. Coloration was stopped by placing the slides in Tris-EDTA (10:1) buffer pH = 7.5 for 10 min.

Sections were imaged at ×40 magnification with a MIRAX MIDI scanner (Carl Zeiss, Oberkochen, Germany). Images were visualized and selected using Mirax Viewer software (3D HISTECH, Budapest, Hungary). Image preparation and assembly were performed in Photoshop CS5 and Adobe Illustrator CS5 (Adobe Systems, San Jose, CA). Images selected for figures had minor adjustments to their brightness to facilitate viewing.

2.6 | Dextran-conjugated dye injection and microscopy

Brain slices were prepared as described in Harvey-Girard et al. (2010, 2013). Four fish were anesthetized with 0.2% MS222 in oxygenated water. Their brains were cut in a transverse manner in the rostral part of mesencephalon (level T 18-T 20; Maler et al., 1991), and the electrosensory nerves were sectioned without pulling brain tissue to avoid structural damage. The caudal brain portion was immersed in ice-cold artificial cerebrospinal fluid (aCSF containing in mM: 124 NaCl, 3 KCl, 0.75 KH_2PO_4, 2 $CaCl_2$, 1.5 $MgSO_4$, 24 $NaHCO_3$, and 10 D-glucose), and embedded in 2.5% agarose/aCSF suspension. Total of 500 μm thick transverse slices of rhombencephalon containing the ELL and the octavolateral efferent (OE) nucleus (sections T −4 to T −5 in the *A. leptorhynchus* brain atlas by Maler et al. (1991)), and of mesencephalon containing nucleus praeeminentialis (nP; sections T 4 to T 10 in Maler et al. (1991)) were sectioned on a vibratome and placed in an electrophysiology chamber at RT and perfused with oxygenated aCSF (95% O_2 and 5% CO_2).

The injection pipette was connected to a stimulation unit driven by a TTL pulse from an Axon Axoclamp 900A Amplifier (Molecular Devices, Sunnyvale, CA) using pClamp 10 (Molecular Devices). Dextran-conjugated tetramethylrhodamine (10 mg/ml; Mini-Ruby, Life Technologies, Waltham, MA) in aCSF was electrically injected (pulses of 100 V lasting 400 ms) in ELL or nP using several pulses at several locations to maximize the injection volume in ELL and nP. Brain slices were perfused in oxygenated aCSF for 4 h to allow dextran transport in neurons. Slices were then fixed overnight in 4% PFA in PBS (pH 7.2). After rinsing twice for 10 min in PBS, the SeeDB clearing protocol (Ke et al., 2013) was applied. In brief, half-day incubation in ascending fructose concentrations in PBS (20% [wt/vol], 40, 60, and 80%) containing 0.5% α-thioglycerol (Sigma-Aldrich, St. Louis, MO) was followed by 24-h incubations in 100% (wt/vol) and 115% (wt/vol) fructose/PBS solutions containing 0.5% α-thioglycerol.

Z-stack images of the thick brain slices were taken using AxioObserver.Z1 microscope (Zeiss). The fluorescent and bright-field images were acquired using AxioVision (Zeiss) on Windows 7. Fluorescent images were processed with the Fiji suite to reduce background. Bright-field and fluorescent images had minor brightness adjustments to facilitate viewing. Z-stack images were transformed to 2D images using the maximum intensity z-projection method from the Image-J software. Final assembly of the merged bright-field and fluorescent images was performed in Photoshop CS5 by overlapping the bright and fluorescent fields and using the superposition of the blend mode. The anatomical levels chosen for these experiments—based on the atlas by Maler et al. (1991)—were T −9 for the ELL (Figure 7), T 8 for the anterior part of the nP (Figure 8), and T 4 for the more posterior aspect of the nP (Figure 9).

2.7 | Ex vivo DiI tracing and 3D reconstructions

Brains from *A. leptorhynchus* were perfused with 4% PFA and collected as described above (N = 22). After 2–4 weeks postfixation at 4°C, the target brain regions where the dye was placed (i.e., ELL and nP) were exposed through vibratome sectioning (brains were sectioned until either target region was reached).

DiI (1,1′-dioctadecyl-3,3,3′,3′-tetramethylindocarbocyanine perchlorate; product #42364, Sigma-Aldrich) and NeuroVue (NeuroVue Jade Solid, product #25687-1, Polysciences) crystals were suspended in 90% ethanol and deposited on a steel needle. This was achieved by dipping the needle in the EtOH-dye suspension before letting it dry in a light-shielded container for about 15 min. With the aid of fine forceps, single dye crystals were collected from the needle and placed onto the brain surface (on a sectioned area corresponding to either ELL or nP) under a stereomicroscope (Leica S9D) to visually localize the target areas. Dye crystals were left in place for about 5 min to facilitate the dye adherence to the tissue. The application site was then sealed by a drop of melting 2% agarose. After this treatment, brain tissues were submerged in fresh 4% PFA and stored at RT

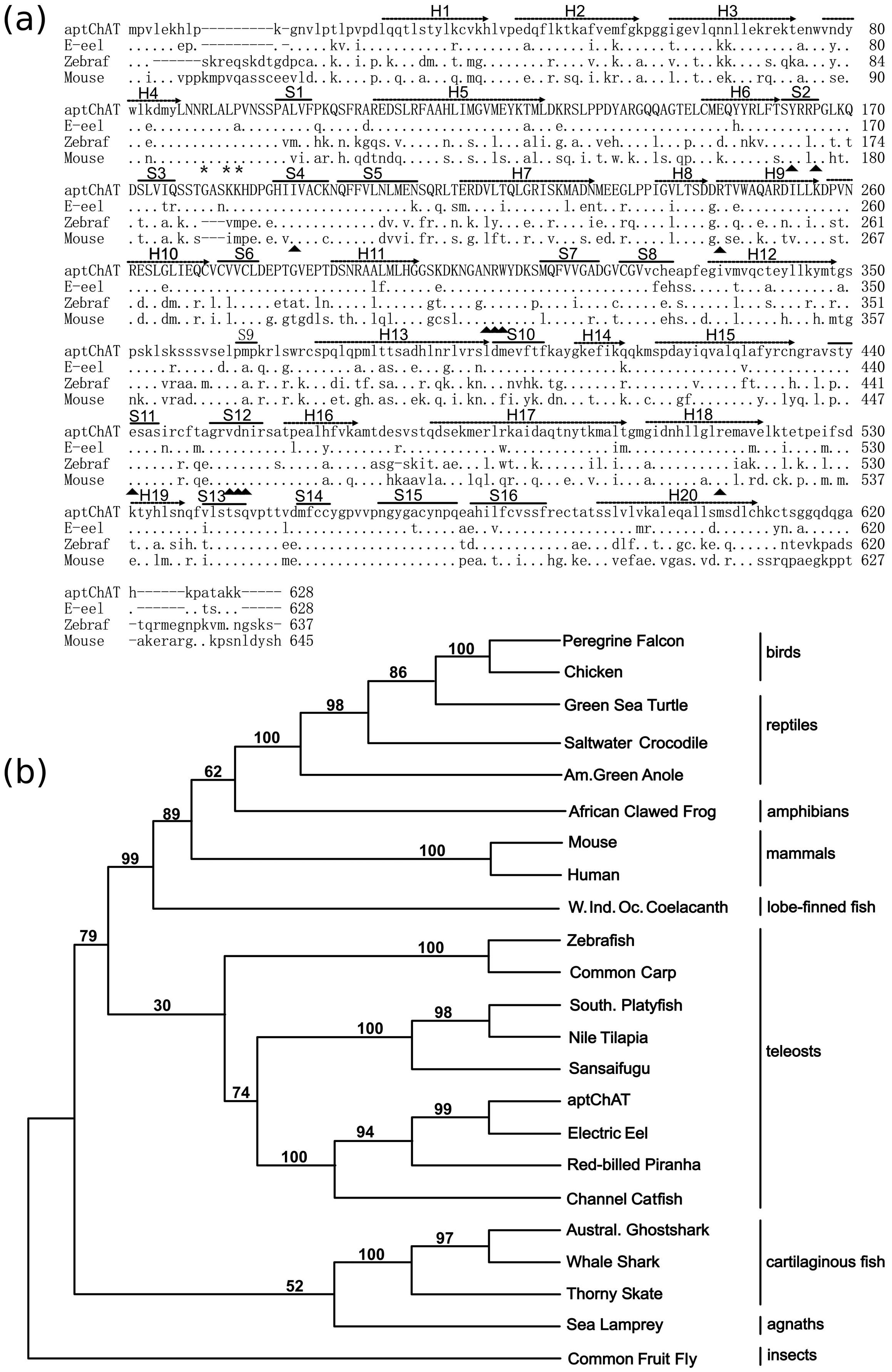

FIGURE 1 Legend on next page.

(ca. 20°C) to allow the passive diffusion of the dye through fiber tracts, from the application site to the rest of the tissue. The 3D reconstruction of DiI-stained tracts and brain areas was carried out 2–4 weeks later, following previously described methods (Oboti et al., 2018). Briefly, dye-stained brains were cut using a vibratome in serial coronal sections (50 μm) and mounted on glass slides. Images from these sections were digitally acquired, postprocessed, and uploaded into ImageJ for alignment and registration (TrakEM2 plugin for FiJi, https://imagej.net/TrakEM2). The 3D morphology of DiI-stained fibers was captured by 2D contour delineation of red fluorescent areas on each section. Importing of the 3D assembly into the open source software Blender (Blender.org) allowed the editing of shading, transparency, and lighting.

Refer to Supplementary Table S1 for a complete list of the in vivo and ex vivo tracing experiments performed.

3 | RESULTS

We partially cloned a segment of the ChAT gene from *A. leptorhynchus* whole-brain cDNA using degenerate primers targeting a region that we found to be conserved in various teleosts. The PCR product resulted in a 730 bp long sequence. To verify this PCR cDNA sequence, we blasted it against the newly published transcriptome shotgun assembly (TSA) from *A. leptorhynchus* in GeneBank (Salisbury et al., 2015). Our PCR cDNA sequence identified several TSA contigs from which we could build a transcript assembly showing an open reading frame of 1887 bps (629 amino acids), which displayed high homology to transcripts from electric eel, zebrafish, and mouse. The PCR fragment sequence fell between the first and the seventh sheet according to the reported mouse ChAT structure (Govindasamy et al., 2004) as shown in capitalized letters in Figure 1(a).

When compared by ClustalW alignment, the *Apteronotus* ChAT (aptChAT) amino acid sequence showed high homology with several known ChAT protein sequences. The predicted protein sequence had an amino acid similarity of 86.6% with its electric eel ortholog, 65.4% with zebrafish ChAT, and 60.7% with its murine ortholog (Figure 1(a)). Amino acids known to lower enzyme activity and substrate specificity when mutated and residues that are thought to be important in the catalytic action (Cronin et al., 2000; Govindasamy et al., 2004; Ohno et al., 2001) were found to be perfectly conserved in aptChAT (Figure 1(a); black triangles and asterisks). These results suggest conserved functional activity of ChAT between teleosts and mammals. Phylogenetic analysis confirmed that the sequenced cDNA fragment is ChAT when we compared it with other ChAT homologs from a wide range of species (Figure 1(b)).

3.1 | Distribution of aptChAT transcripts

The expression of aptChAT transcripts in the brain of *A. leptorhynchus* was analyzed by in situ hybridization in transverse sections of the brain. The nomenclature used is based on Maler et al. (1991).

Intense positive signals showing expression of ChAT mRNA were restricted to the perikaryon of cells in various nuclei throughout the fish brain. The ChAT sense probe did not label any cells in spinal cord or brain (Figure 3(a)). We divide the description of the ChAT-positive nuclei in motor and nonmotor nuclei, and further divide the nonmotor nuclei according to their locations in the brain.

3.2 | Motor nuclei

Sections from the midbrain (tectal and isthmic areas), hindbrain, and medulla of *A. leptorhynchus* were examined. Labeled cells were found in several motor nuclei from rostral to more caudal levels.

The oculomotor nucleus (nIII) appears as an intensely labeled group of neurons in the most medial part of the mesencephalon (Figure 2(a)). This nucleus shows similar appearance and location to that reported in other fishes, in which it has been described as cholinergic (Adrio et al., 2000; Anadón et al., 2000; Clemente et al., 2004; Mueller et al., 2004; Pérez et al., 2000). The trochlear nucleus (nIV), located close to the midline of the rhombencephalon, next to the ventricle, also showed strong staining (Figure 2(b)). The abducens nucleus was, for unknown reasons, not clearly detected in our samples.

Positive cells were also seen in the facial motor nucleus (nVIIm; Figure 3(a)) and the motor trigeminal nucleus (nVm; Figure 3(b)). Some ChAT-labeled cells with large soma were scattered in the paramedian reticular formation (PRF) area, lateral to the medial longitudinal fasciculus (MLF; Figure 3(b,c)). From here toward more caudal positions, the spinal motor column (smc) is seen throughout the medulla oblongata, as well as expression of ChAT transcripts in cranial nerve motor nuclei (Maler et al., 1991). The vagal motor nucleus (nXm) and possibly the glossopharyngeal nucleus (nIXm) appear continuous, as part of the spino-occipital motor neurons. They are located periventricular at different levels of the rhombencephalon in the transverse sections

FIGURE 1 Sequence alignment and phylogenetic tree of choline acetyltransferase. (a) Predicted amino acid sequence of *Apteronotus leptorhynchus* choline acetyltransferase (aptChAT) aligned against electric eel, zebrafish and mouse ChAT orthologs. Identical amino acids to aptChAT are shown as dots. Capitalized letters display the sequence location of the in situ RNA probe. The secondary structural elements are based on the structure of rat ChAT taken from Govindasamy et al. (2004). The sheets and helices are identified by solid and dashed horizontal arrows, respectively. Conserved amino acid residues, where deleterious point mutations have been identified for the rat ChAT, are identified by asterisks. Residues that are thought to be important in the catalytic action are identified by black triangles (Cronin et al., 2000; Govindasamy et al., 2004; Ohno et al., 2001). (b) Phylogenetic tree of the partial aptChAT protein sequence compared to protein sequences from 21 vertebrate species and common fruit fly as an outgroup. Numbers in the phylogeny tree provide confidence level for each branch. Species were chosen to include representatives of each major vertebrate clade. Teleostei are over-represented to classify aptChAT better

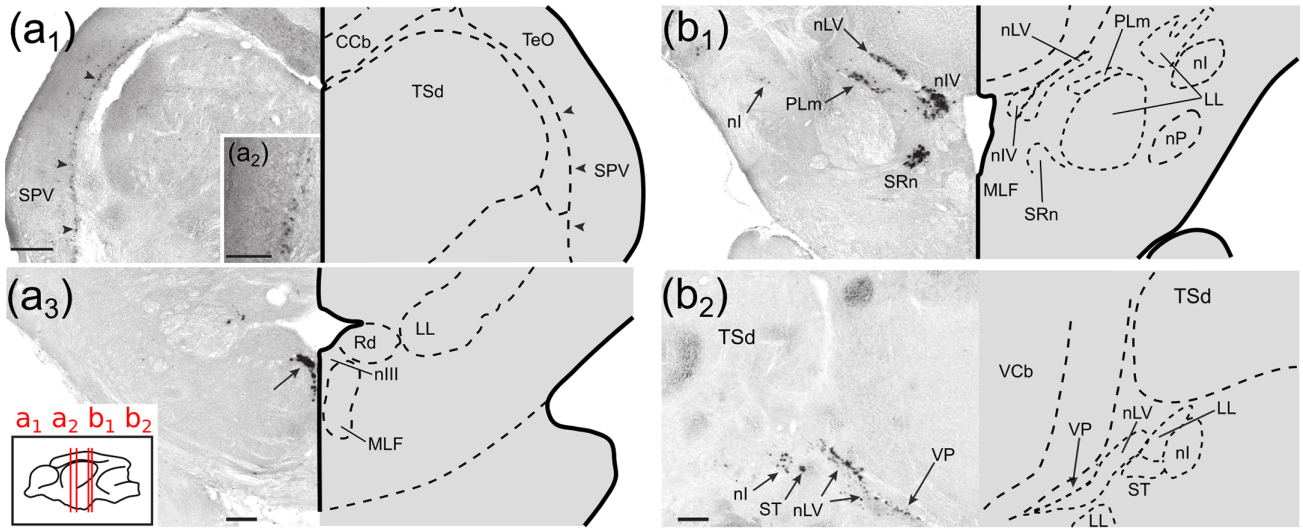

FIGURE 2 In situ hybridization of *Apteronotus leptorhynchus* choline acetyltransferase (aptChAT) antisense mRNA probe of transverse sections of the mesencephalon of *A. leptorhynchus*. (a1) aptChAT mRNA labeling is observed in the stratum periventriculare (SPV) of the optic tectum (TeO). Insert in (a1) high magnification of the cells in SPV. They appear in small clusters along the entire length of SPV (arrowheads, a2). (a3) aptChAT mRNA labeling is densely present in the oculomotor nucleus (nIII). (b1) in a more caudal section, the strongly labeled trochlear nucleus (nIV) can be seen periventricular and medial to the lateral lemniscus (LL). Ventral to nIV, the superior reticular nucleus (SRn), a sub-nucleus of the reticular formation, is also labeled. In addition to the moderate number of cells labeled in nucleus isthmi (nI), two relatively densely stained nuclei are present in the isthmic area. The more medial and dorsal one corresponds to the nucleus lateralis valvulae (nLV), the second one may correspond to the medial subdivision of the perilemniscal nucleus (PLm), or a second branch of nLV; based on in situ hybridization only, we are unable to determine their exact identity. (b2) labeling in the isthmic area is also seen in a slightly more posterior section, ventrolateral of the valvular peduncle (VP) (arrow). A dense cluster of cells medial of nI may correspond to the subtoral nucleus (ST). The hemisections on the right of each panel outline the structures contained in the mirror-image brain sections. The insert at the bottom of (a2) shows the positions of the transverse sections in a schematic side view of the apteronotid brain ((a1) = T 14, (a2) = T 13, (b1) = T 8, (b2) = T 7, as in Maler et al. (1991)). Scale bars: 100 μm [Color figure can be viewed at wileyonlinelibrary.com]

(Figure 3(b–e)). A group of large ChAT-positive cells, corresponding to the motor column, was present in the ventral horn of the spinal cord extending from the ventral part and reaching the area lateral to the MLF (Figure 3(f)). No labeling was observed at more caudal levels (Figure 3(g)).

3.3 | Nonmotor nuclei

3.3.1 | Prosencephalon

The telencephalon showed a sparse distribution of cholinergic neurons. ChAT-positive cells were only found in subpallium and other ventral telencephalic areas (Figure 4); labeled cells were completely absent from the pallium. Most of the cell bodies of the labeled neurons were small and organized in small clusters. The most intense labeling was found in the ventral zone of the ventral telencephalon (VVv; Figure 4(a,c)). Dorsolateral to this cell cluster, small cell bodies of the medial olfactory terminal field (MOTf; Sas et al., 1993) showed ChAT mRNA expression (Figure 4(a,b)).

In the preoptic region, we identified two groups of ChAT-positive cells. A first group was located in the posterior subdivision of the preoptic nucleus (PPp), which lies dorsal to the suprachiasmatic nucleus (Sc; Figure 4(d,e)). We also found positive staining for ChAT mRNA transcripts in a more posterior nucleus, dorsal to the Sc and ventral to the anterior hypothalamic nucleus (Ha), denoted as nucleus anterior periventricularis (Figure 4(f,g)). Interestingly, although in most other vertebrates the habenula has been observed to contain ChAT-positive neurons, we did not find ChAT-positive cells in the habenula of *A. leptorhynchus*, as reported for other teleost species (Casini et al., 2018; Clemente et al., 2005; Ekström, 1987).

3.3.2 | Mesencephalon and rhombencephalon

Within the mesencephalon and the rhombencephalon, cells expressing ChAT transcripts are present in the optic tectum (TeO), the isthmic area, and the region of the OE nucleus.

In the TeO, ChAT-positive perikarya were found exclusively in the stratum periventriculare (SPV; Figure 2(a_1) and insert), where they were arranged in small clusters of three to four cells. The SPV of *Apteronotus* (Sas & Maler, 1986b) and other teleosts (Meek & Schellart, 1978) is densely packed with small neurons, and it is therefore clear that only a relatively limited subset was ChAT-positive.

The region showing the most numerous and intensely stained neurons labeled with the ChAT antisense probe was in the isthmic region. Besides the discrete group of medium-sized cells just ventral to the torus semicircularis (TS), corresponding to nucleus isthmi (nI;

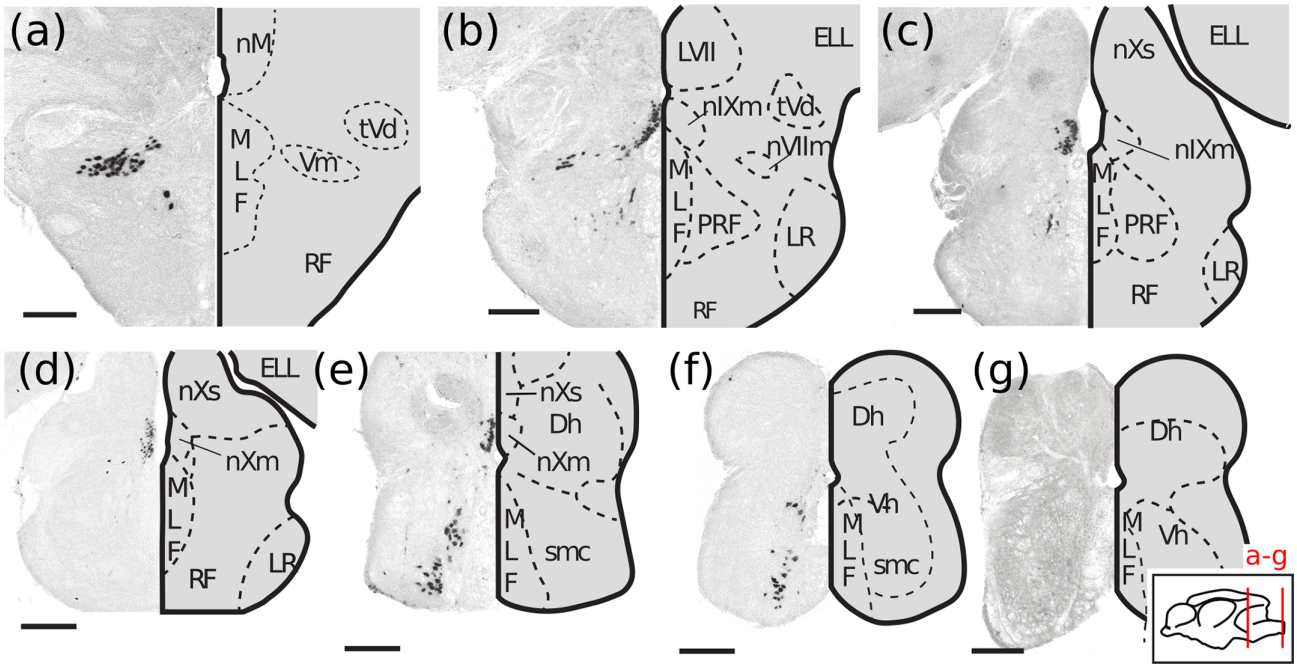

FIGURE 3 In situ hybridization in transverse sections of *Apteronotus leptorhynchus* spinal cord and medulla with the *A. leptorhynchus* choline acetyltransferase (aptChAT) sense RNA probe (g) and the antisense RNA probe (a–f). Whereas the aptChAT sense RNA probe did not stain the tissue (a), the aptChAT antisense RNA probe resulted in intense labeling of motoneurons of the spinal motor column (smc) (b,c). Neurons of the motor part of the vagal nucleus (nXm) and the glossopharyngeal nucleus (nIXm) were labeled at various levels of the medulla (c–f). (f) Label was also found in neurons of the facial motor nucleus (nVIIm). (g) Positive cells were also seen in the motor trigeminal nucleus (Vm). The hemisections on the right of each panel outline the structures contained in the mirror-image brain sections. Insert in (a) shows the positions of the transverse sections in a schematic side view of the apteronotid brain ((a) = T −5, (b) = T −11, (c) = T −12, (d) = T −13, (e) = T −14, (f,g) = posterior to T −14 (not represented in the atlas by Maler et al. (1991)). Scale bar: 100 μm [Color figure can be viewed at wileyonlinelibrary.com]

Figure 2(b_1,b_2)), other intensely labeled cell clusters were present in what is likely to be the subtoral nucleus (ST; Figure 2(b_2)). Other cells extended medioventrally from TS to the rostral part of nIV and likely belong to the nucleus lateralis valvulae (nLV; Figure 2(b_1)). Ventral to these cells lies a string of stained neurons that may be part of a second branch of nLV or the medial paralemniscal nucleus (PLm; shown to be cholinergic in zebrafish; Clemente et al., 2004; Mueller et al., 2004). Since our approach did not permit fiber staining, we cannot use connectivity as a criterion for a more conclusive identification of these cell clusters.

The last region in the midbrain showing ChAT mRNA expression consisted of a dense cluster of cells ventromedial of the lateral lemniscus (LL; Figure 2(b_1)). It is likely that these cells belong to the superior reticular nucleus (SRn), which lies just ventromedial to the LL in zebrafish and has been shown to be cholinergic (Clemente et al., 2004; Wullimann et al., 1996). SRn has been suggested to be homologous to the cholinergic laterodorsal tegmental area in mammals (Mueller et al., 2004).

In the rhombencephalon, cells expressing aptChAT transcript were found lateral to the MLF just under the ventricle, in the area where the OE has been described in other teleosts (Figure 5(a); Danielson et al., 1988; Clemente et al., 2004). Labeling was also seen in large cells of the PRF at this level.

3.4 | Sources of ACh released in electrosensory nuclei

In previous work, we localized the expression of muscarinic receptors (mAChR) in *A. leptorhynchus* brain. The receptors were expressed in many nuclei throughout the brain including dorsal telencephalon and hypothalamic areas. Interestingly, various nuclei devoted to electrosensory information processing were positive for mAChR including the ELL, nP, TS, and TeO (see Figure 11 for summary; Toscano-Márquez, Dunn, & Krahe, 2013).

We sought to identify the source of cholinergic innervation arriving at two key electrosensory nuclei, nP and ELL. ELL is the first stage of central nervous processing of electrosensory information. It projects to nP, which provides feedback to ELL via several routes (Bell & Maler, 2005). Eurydendroid cells located at the ventral limit of the eminentia granularis posterior (EGp) had been suggested to be cholinergic (Maler et al., 1981; Sas & Maler, 1987) and to provide modulatory input to ELL via vertical fibers (Berman & Maler, 1999). Interestingly, these eurydendroid cells turned out not to be labeled by our ChAT antisense probe (Figure 5(b)), indicating that these cells are not cholinergic and that the cholinergic inputs to ELL come from another source, contrarily to what had previously been hypothesized (Maler et al., 1981).

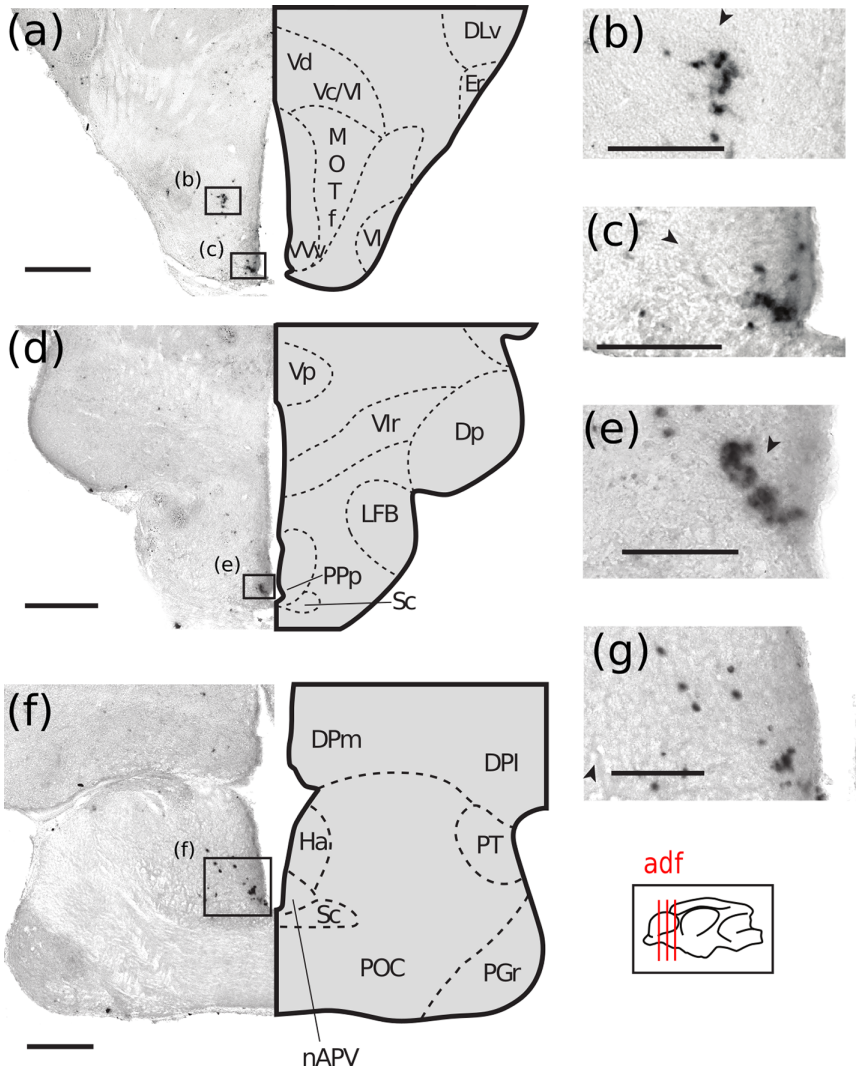

FIGURE 4 In situ hybridization of *Apteronotus leptorhynchus* choline acetyltransferase (aptChAT) antisense mRNA probe of transverse sections of the telencephalon. (a) Strong and highly localized aptChAT mRNA labeling is observed in the most ventral zone of the ventral telencephalon (VVv) and in the medial olfactory terminal field (MOTf). (b) Close-up of the labeled neurons in MOTf. (c) Close-up of the labeled neurons in VVv. (d) A more caudal section of the telencephalon on the border of the diencephalon with labeling of aptChAT mRNA in the ventral part of the posterior subdivision of the preoptic nucleus (PPp). (e) Close-up of the labeled neurons in PPp. (f) High-magnification view of labeled neurons in the nucleus anterior periventricularis (nAPV) shown at lower magnification in (g). The hemisections on the right of each panel outline the structures contained in the mirror-image brain sections. Insert in (a) shows the positions of the transverse sections in a schematic side view of the apteronotid brain ((a–c) = T 33, (d) = T 29, (g) = T 27). Scale bars: 100 μm [Color figure can be viewed at wileyonlinelibrary.com]

To determine the source of ACh to ELL we performed injections of dextran-conjugated tetramethylrhodamine (mini-Ruby 10.000 MW) in thick brain slices, because in vivo injections in ELL risk leakage into the dorsally adjoining EGp, which is heavily connected to many parts of the brain (Sas & Maler, 1987). The transverse slices included the sections T −4/−5 of the rhombencephalon as defined in the atlas of the *A. leptorhynchus* brain (Maler et al., 1991) using the rostral aspect of the pacemaker nucleus (not shown) to visualize the level containing OE. We found a bundle of labeled axons that started in OE and crossed the midline immediately after leaving OE and then followed a vertical trajectory to the site of injection in the contralateral ELL (Figure 6(a–c)). Unfortunately, clear soma labeling in OE was not achieved. The lack of full soma labeling could be due to difficulties in keeping the slices alive long enough for the dye to fill the neurons sufficiently.

nP is a central feedback nucleus of the electrosensory system and showed a high density of muscarinic receptor mRNA expression (Toscano-Márquez, Dunn, & Krahe, 2013). Given the close proximity of nP and the isthmic region, which showed high expression of ChAT mRNA (Figure 2($b_{1,2}$)), we suspected that it could be the source of cholinergic input to nP. in vivo injections into nP tend to leak dorsally into TS (L. Maler, unpublished data). Therefore, we used a similar transverse slice preparation as above to allow clean injection into nP. Injection in the medial aspect of nP indeed resulted in retrogradely labeled cells in the region of a ChAT-positive cell cluster that lies dorsolaterally adjacent to the LL and medial to nP (Figure 6(d–f)). The thin axons did not travel in an organized bundle, but instead formed net-like projections of which some ended in cell bodies, the precise localization of which could not be easily defined in such thick sections and with so few labeled neurons.

To overcome these limitations and verify the results of the dextran injections, we adopted an ex vivo tracing approach using carbocyanine-based dyes (DiI and NeuroVue, Heilingoetter & Jensen, 2016; Jensen-Smith et al., 2007; Linke et al., 1995; Yoshida et al., 1999). DiI tracing was carried out on fixed brain tissue (see methods) after exposing the target areas (ELL or nP) through vibratome sectioning (Figures 7–9). DiI application on the ELL yielded similar results to our dextran injection experiments: labeled axon terminals in the ELL ventral molecular layer and pyramidal cell layer were traced back to their source in the EO, after decussating at the level of

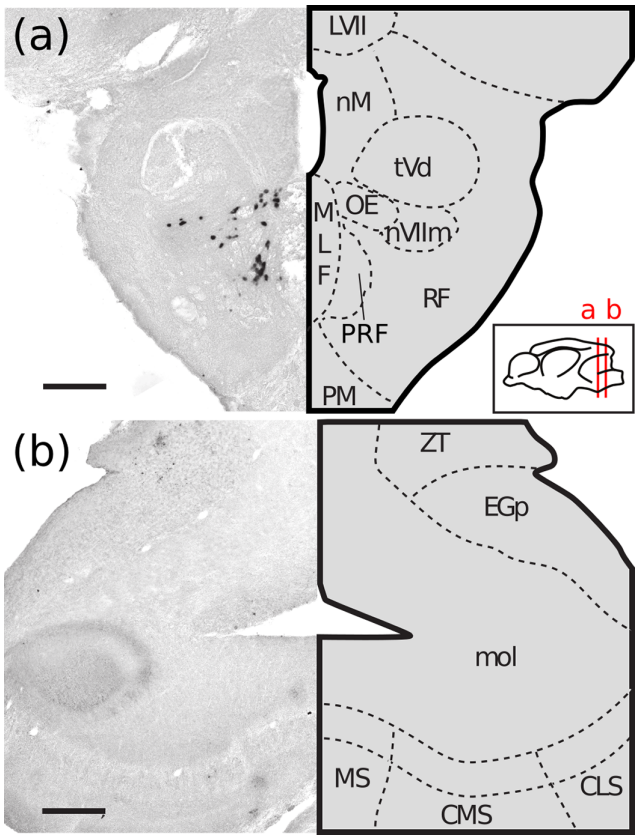

FIGURE 5 In situ hybridization of *Apteronotus leptorhynchus* choline acetyltransferase (aptChAT) antisense mRNA probe in transverse sections of the rhombencephalon of *A. leptorhynchus*. (a) aptChAT-positive labeling of cells of the octavolateral efferent nucleus (EO), the facial motor nucleus (nVIIm) and the nonmotor nucleus of the paramedian reticular formation (PRF). (b) Dorsal part of a transverse section through the rhombencephalon showing the absence of aptChAT mRNA-positive cells in the EGp and ELL regions. The hemisections on the right of each panel outline the structures contained in the mirror-image brain sections. Insert in (a) shows the positions of the transverse sections in a schematic side view of the apteronotid brain ((a) = T −5, (b) = T −9). Scale bar: 100 μm [Color figure can be viewed at wileyonlinelibrary.com]

the commissure of the ELL (cELL), following the same course as the dextran-traced axons (Figure 7(a–e)). Here, cell somata were clearly distinguishable specifically in correspondence to the EO (Figure 7(e)), whereas no labeled neurons were found in adjacent nuclei (Figure 7 (f)). The duration of this tracing experiment (10–15 days) was ideal to assess the presence of cholinergic afferents in the OE and eventually the surrounding hindbrain nuclei; however, it was not well suited to trace other long-range projections possibly belonging to other cholinergic afferents directed to the ELL. Therefore, although this experiment validates our previous biotin tracing approach, it does not rule out the presence of other long-range cholinergic projections from outside the hindbrain.

Tracing from injections in nP (Figure 8(a)) resulted in very intense staining in the areas surrounding the application site (Figure 8(b,c)), including nLV, reticular formation (RF), and LL, suggesting the presence of diffuse interconnections (possibly traced both anterogradely and retrogradely) between the nP and both the ipsilateral and contralateral mesencephalon. Several strongly labeled axons (empty arrowheads in Figure 8(d)) were found departing from the nP and directed toward the dLL, but no stained cell bodies were found (Figure 8(d,e)). Due to the lesser section thickness (50 μm) allowing a clearer spatial separation of the isthmic nuclei, we were able to localize labeled somata more precisely along the rostrocaudal axis, approximately 700–800 μm from the targeted site (Figure 8(f)). Because the isthmic nuclei were localized in close proximity to the often strongly labeled injection sites positioned at this level (T 7-T 8), we performed an additional set of injections at more posterior levels (T 4, Figure 9(a–c)). To further limit the spread of the dye around the injected area, we used a different dye with lower local diffusion and faster tracing times (NeuroVue). In these experiments, dye-labeled cells were found again in the isthmic region, in correspondence of the nLV/PLm area (Figure 9(d–f)). Further, 3D brain reconstruction allowed to trace dye-stained axons across several consecutive and adjacent tissue sections (Figure 10). This allowed to validate our results based on the presence, absence, and coherence of dye-stained tissue when belonging to the same pathway or brain region.

Only few labeled cell bodies were found, which were located in proximity of nI (lateral to the LL and ventral to the TSd; Figure 8(f)) when dye was injected in the nP at the T 7 level. Several labeled cells were found near the dye application site and in the nLV area (Figure 9) when injections occurred at more caudal levels (T 4). Overall, these results indicate that in the hindbrain of weakly electric fish, the OE is an important source of cholinergic innervation of ELL, whereas in the midbrain, the nLV and the nI are likely sources of cholinergic innervation to nP.

4 | DISCUSSION

The aim of this study was to determine the distribution of cholinergic cells in the brain of the weakly electric fish, *A. leptorhynchus*. We first identified ChAT mRNA of *A. leptorhynchus* and then used an in situ hybridization approach to label the cholinergic cells in transverse sections of the brain. This approach combined with injections of retrograde tracer in electrosensory nuclei allowed us to track some of the sources of ACh released in electrosensory nuclei.

As expected, we found ChAT expression in cells belonging to the spinal motor column and the cranial nerve motor nuclei (Figures 2 and 3). In addition, we identified previously undescribed projections from the OE to the ELL, the sole recipient of electrosensory afferents in the hindbrain. We were able to retrogradely label from the nP putative cholinergic projections in the isthmic region, the nI and nLV. The nP is a key feedback nucleus of the electrosensory system: it resides upstream of the ELL and regulates, through several feedback projections, the response properties of ELL pyramidal neurons (Bell & Maler, 2005; Hofmann & Chacron, 2019). Thus, our results imply that cholinergic pathways are involved in central modulatory processes in the higher-order regions of the electrosensory system. In the

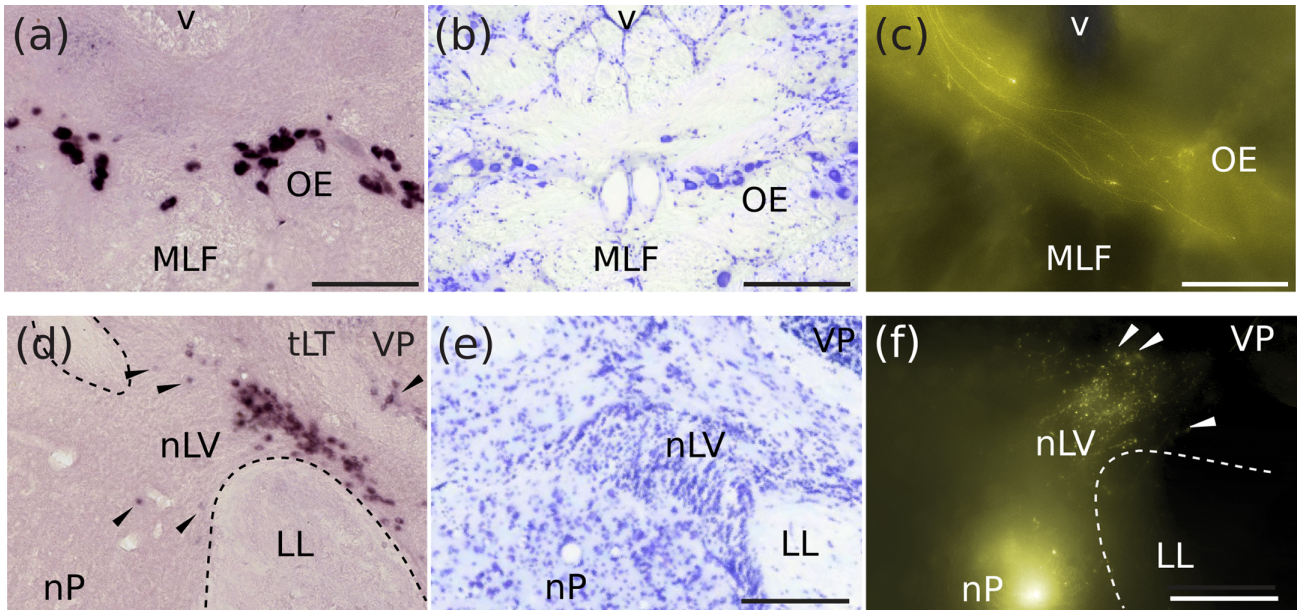

FIGURE 6 Dextran-conjugated tetramethylrhodamine injections into two electrosensory nuclei. (a) In situ hybridization of *Apteronotus leptorhynchus* choline acetyltransferase (aptChAT) at the level of the octavolateral efferent nucleus (OE). (b) Micrograph of an equivalent cresyl-violet-stained section of the rhombencephalon showing the medial longitudinal fasciculus (MLF) in the center of the field, ventral to the ventricle, and the OE on both sides of MLF. (c) Result of the injection of the dextran dye into the molecular layer of the electrosensory lateral line lobe (ELL) (not shown). A bundle of axons leaves the OE, decussating immediately outside of OE and following a vertical trajectory to the site of injection in the contralateral ELL. (d) In situ hybridization of aptChAT at the level of nucleus praeeminentialis (nP) and a part of the nucleus lateralis valvulae (nLV). The arrowheads indicate both clustered and sparse labeling scattered around the area. (e) Micrograph of an equivalent cresyl-violet-stained section as in (d). (f) Labeling resulting from an injection in the medial aspect of nP (showing the migration of the dye from the injection site (bright spot at the bottom) to axons and a few cell bodies in the area of nLV (arrowheads). Positions of the transverse sections in the apteronotid brain are (a–c) = T −5, (d–f) = T8). Scale bar: 200 μm [Color figure can be viewed at wileyonlinelibrary.com]

following, we will first briefly compare the sequence data for aptChAT with ChAT sequences known from other species and then place our anatomical findings in their larger context of brain connectivity and possible function.

4.1 | Comparison of aptChAT with ChAT sequences from other species

The amino acid sequence of aptChAT is highly conserved between mammals, other teleosts, and *A. leptorhynchus*. Functional residues identified based on the mouse ChAT (mChAT) are known to be part of the acetyl-CoA binding site (Govindasamy et al., 2004). Specifically, point mutations in mChAT Leu102, Pro103, Ile197, and Arg312, which lead to decreased affinity to acetyl-CoA, and point mutations at Glu441, which lack catalytic activity, have been linked to congenital myasthenic syndrome with fatal episodes of apnea in humans (Ohno et al., 2001). All of these identified point mutation sites are conserved in aptChAT as well as the other teleosts included in our comparison (Figure 1(a)). The His334 residue that has been shown to be the catalytic site of ChAT (Govindasamy et al., 2004) was apparently lost in apteronotid and zebrafish orthologs, but is present in electric eel. Other residues, such as Arg250, Asn311, Arg312, and Trp313 that are hypothesized to interact with the catalytic site of ChAT, were found to be conserved in aptChAT. Finally, four amino acid residues involved in the choline/carnitine binding specificity, VDN453-455 and E441, are also conserved (Cronin et al., 2000). All these results suggest a strong conservation of functional features of ChAT activity in all vertebrates.

4.2 | ChAT-positive elements in the forebrain of gymnotiform weakly electric fish

In the light of recent studies that revealed several homologies between pallial and subpallial areas in fish and mammals (Briscoe & Ragsdale, 2019; Ganz et al., 2012; Giassi, Duarte, et al., 2012; Giassi, Ellis, & Maler, 2012; Giassi, Harvey-Girard, et al., 2012; Harvey-Girard et al., 2012; Nieuwenhuys, 2009; Wullimann & Mueller, 2004), it is worth mentioning that, in areas ascribed to the dorsal telencephalon (Giassi, Duarte, et al., 2012; Giassi, Ellis, & Maler, 2012; Giassi, Harvey-Girard, et al., 2012; Harvey-Girard et al., 2012), no ChAT-positive cells were detected. This situation is similar to that described for the pallium of most other fish species (Lopez et al., 2012; López et al., 2013; Morona et al., 2013; Mueller et al., 2004). As in these studies, cholinergic cells were restricted to the ventral telencephalic areas of *A. leptorhynchus*, where we found small groups of ChAT-positive cells only in the VVv and the MOTf area (Figures 4 and 11).

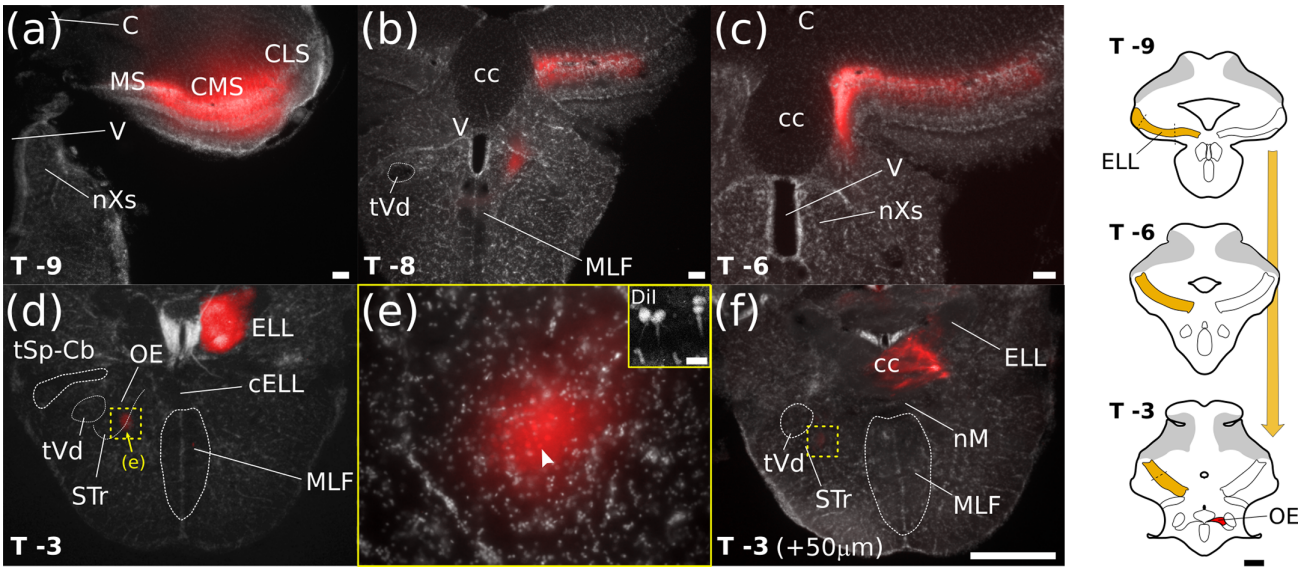

FIGURE 7 Photomicrographs and reconstructions of carbocyanine-based dye (DiI and NeuroVue) applications onto the ELL (a–f). (a–e) Serial tissue sections (from posterior to anterior) showing DiI-stained fibers coursing toward progressively anterior levels (from T-9 to T-3, as in Maler et al. (1991); adjacent T levels are ca. 150 μm apart). A small bundle of fibers is decussating at the level of the cELL, toward the contralateral hemisphere (T3, f) and ends in the OE. (d,e) Retrogradely DiI-stained fibers and nuclei in the OE (higher magnification of the boxed area in panel d). (f) DiI-stained cell bodies are not visible (only a few fibers) in the corresponding area on the adjacent tissue section (50 μm apart, see boxed area in f). The panels on the upper right show the localization of dye application (orange). The arrows indicate the location of the application sites and the direction of dye transport. The areas in which labeled cells were found are shown in red. Scale bars: 500 μm (diagram), 100 μm (a–f), 15 μm (insert in e). Since image acquisition was set to detect the minimum labeling intensity in the specimen and kept constant across all section, the dye application sites appear overexposed [Color figure can be viewed at wileyonlinelibrary.com]

The VVv has been identified as a septal region (Ganz et al., 2012; Mueller et al., 2008; Wong, 1997). The connectivity of the teleost VVv and the septal nuclei of other vertebrates have striking similarities. VVv expresses high levels of cannabinoid receptor transcripts, similar to septal cholinergic cells in mammals (CB1R; Harvey-Girard et al., 2013). Like the septal nuclei of other vertebrates, it is heavily connected with the preoptic area and hypothalamic nuclei (Wong, 1997). Moreover, in the gymnotiform weakly electric fish, *Eigenmannia virescens*, VVv connects with nucleus electrosensorius (nE), a nucleus known to be critical to processing of electrocommunication signals (Heiligenberg et al., 1991; Wong, 1997). All the known targets of VVv express at least one type of muscarinic receptor in *A. leptorhynchus* (Figure 11; Toscano-Márquez, Dunn, & Krahe, 2013). Thus, our present results confirm VVv as a septal region and suggest that it modulates detection of, and responses to, electrocommunication signals via muscarinic receptors.

The MOTf is a terminal field of olfactory bulb efferents (Sas et al., 1993) associated with dorsal (Vd), central (Vc), and intermediate (Vi) parts of the subpallium (Figures 4 and 11; Harvey-Girard et al., 2013; Sas & Maler, 1987; Sas et al., 1993). Several studies have suggested that this subpallial area is homologous to the striatum or, perhaps more specifically, ventral striatum (Ganz et al., 2012; González et al., 2014; Harvey-Girard et al., 2013; Sas et al., 1993). The ChAT-positive cells in the MOTf might therefore be considered homologous to ventral striatal cholinergic neurons. The functional role of these telencephalic cholinergic neurons (VVv and MOTF) may be the activation/modulation of the teleost fish pallium and diencephalon, similar to the cholinergic populations of the basal forebrain in tetrapods (de Almeida et al., 2016; Dutar et al., 1995; Ericsson et al., 2011; Smith et al., 2015; Stephenson-Jones et al., 2012).

The posterior subdivision of the preoptic nucleus (PPp) was ChAT-positive (Figures 4 and 11. Cholinergic cells in the preoptic region have been reported previously in the trout (Pérez et al., 2000), zebrafish (Clemente et al., 2004; Mueller et al., 2004), and in a chondrostean (Adrio et al., 2000). In gymnotiform fish, PPp connects to the suprachiasmatic, preglomerular (PG), and hypothalamic nuclei (Giassi, Duarte, et al., 2012), which express different muscarinic receptor types (Toscano-Márquez, Dunn, & Krahe, 2013).

4.3 | ChAT-positive elements in mesencephalon and rhombencephalon

4.3.1 | Cholinergic neurons of the isthmic region

The most prominent cholinergic population in the brain of *A. leptorhynchus* was located in the mesencephalic isthmic region, ventral to TSd and medial to nP and LL (Figure 2(b_1,b_2)). This area has been found to contain very high ChAT levels also in other teleosts (Clemente et al., 2004; Contestabile et al., 1979; Mueller et al., 2004; Pérez et al., 2000). It comprises several nuclei including the nI, nLV, and the medial paralemniscal nucleus (PLm).

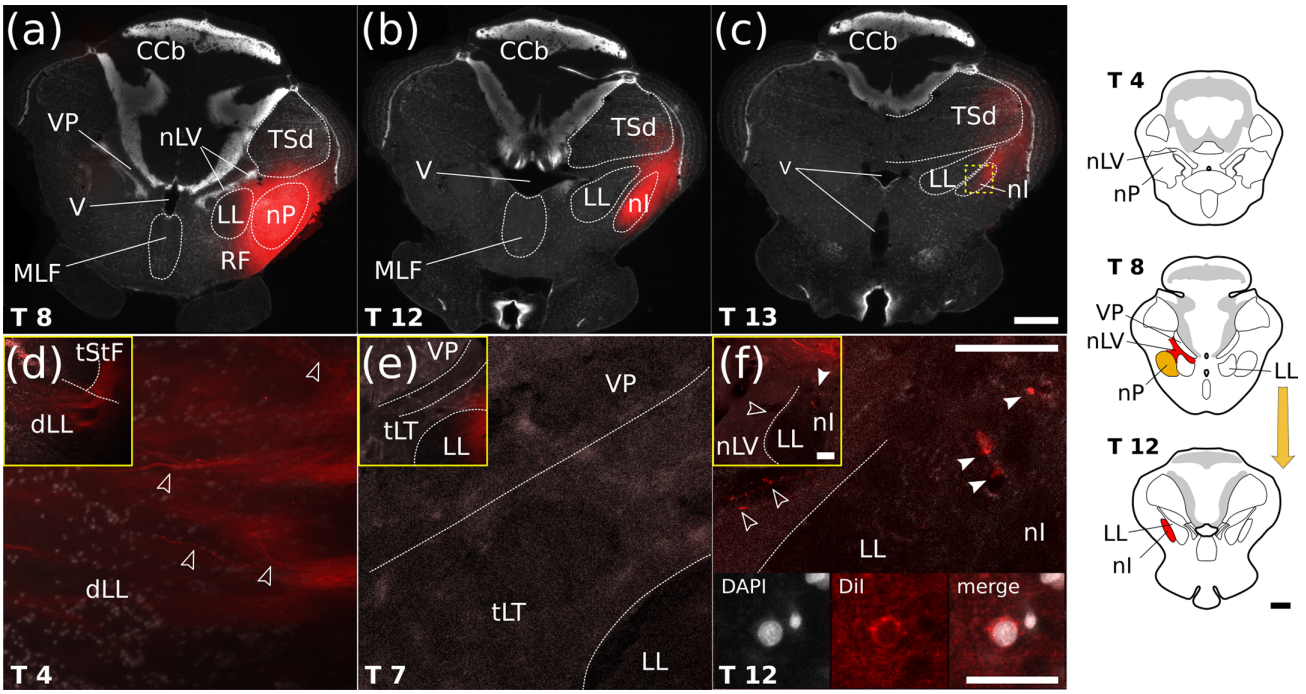

FIGURE 8 Photomicrographs and reconstructions of carbocyanine-based dye (DiI and NeuroVue) applications onto the anterior nP (a–f). (a–c) Serial tissue sections (from posterior to anterior) showing DiI-labeled fibers coursing from posterior (T 8) to progressively anterior levels (T 13). While most of the stained axons seem to progress rostrally toward the nl (a–c), several isolated DiI-stained processes were found in proximity to the injection site directed toward the dLL (arrowheads in d). However, no DiI-stained somata were found at this level (T 4, d) or at the level of the tLT (T 7, e), whereas a few DiI-stained cells were visible in the nl (T 12, f). The panels on the upper right show the localization of dye application (orange). The arrows indicate the location of the application sites and the direction of dye transport. The areas in which labeled cells were found are shown in red. Scale bars: 500 μm (diagram), 100 μm (a–f), 15 μm (details of double positive cell in f). Since image acquisition was set to detect the minimum labeling intensity in the specimen and kept constant across all section, the dye application sites appear overexposed [Color figure can be viewed at wileyonlinelibrary.com]

The cholinergic part of nl in fish and birds is homologous to the parabigeminal nucleus of mammals (Diamond et al., 1992; Wang et al., 2006; Xue et al., 2001). It is located ventral to the TSd and dorsomedial to the nP (Sas & Maler, 1986a), but varies greatly in size in different species (Pérez et al., 2000; Zottoli et al., 1988). The nl is considered to be a visual center in non-electroreceptive teleosts (Northmore, 1991; Wang, 2003). It is interconnected with the tectal formation by feedback loops, which can involve both the ipsi- and the contralateral tectum, depending on the species. The nl has been functionally implicated in the detection of looming stimuli in goldfish and other species (Gallagher & Northmore, 2006), while studies conducted in zebrafish attributed to it a role in the sensory gating of visual inputs (role in *object movement detection*; Fernandes et al., 2019) and in the sustained visual tracking of prey (Henriques et al., 2019).

The nLV has been considered to be a relay of sensory information to the cerebellum (Yang et al., 2004). The combination of our in situ hybridization and tracing experiments suggests the presence of cholinergic afferents to the nP originating in the nLV (Figures 2(b) and 9(a, b)). In teleost fishes, nLV receives lateral line inputs as well as retinotopic and somatotopic inputs from trigeminal nuclei (Ito & Yoshimoto, 1990; Xue et al., 2005). It relays sensory information mainly to the valvula and corpus cerebelli including eurydendroid cells in tilapia, but reciprocal projections to the inferior lobe have also been shown (Ahrens & Wullimann, 2002). Although not much is known about the function of nLV, it has been suggested to be homologous to some of the pontomesencephalic nuclei in mammals based on its position and connections (Imura et al., 2003; Oda, 1999). These nuclei play an important role in arousal as part of the reticular activating system, cardiovascular and respiratory control, and modulation mechanisms controlling gait and posture (Jones, 2003; Martinez-Gonzalez et al., 2011).

However, recent studies on the connectivity and neurochemical phenotype of the cells of the isthmic region have suggested that the identity of nLV as a cholinergic nucleus should be revisited, and the cholinergic cells of that region should be considered instead part of the secondary gustatory and visceral nucleus (SG/V), which has previously been shown to be cholinergic (Castro et al., 2006; Mueller et al., 2004; Yáñez et al., 2017). The SG/V area is very prominent in teleosts and consistently found to send cholinergic projections coursing through the ventral midbrain to the RF, thalamus, and hypothalamus (Mueller et al., 2004; Pérez et al., 2000; Yáñez et al., 2017). Nonetheless, both, because the exact location of the SG/V in the brain of *A. leptorhynchus* is still not clear, but also due to the debated presence of cholinergic neurons in the nLV (Castro et al., 2006; Clemente et al., 2004; Mueller et al., 2004), we have decided to assign

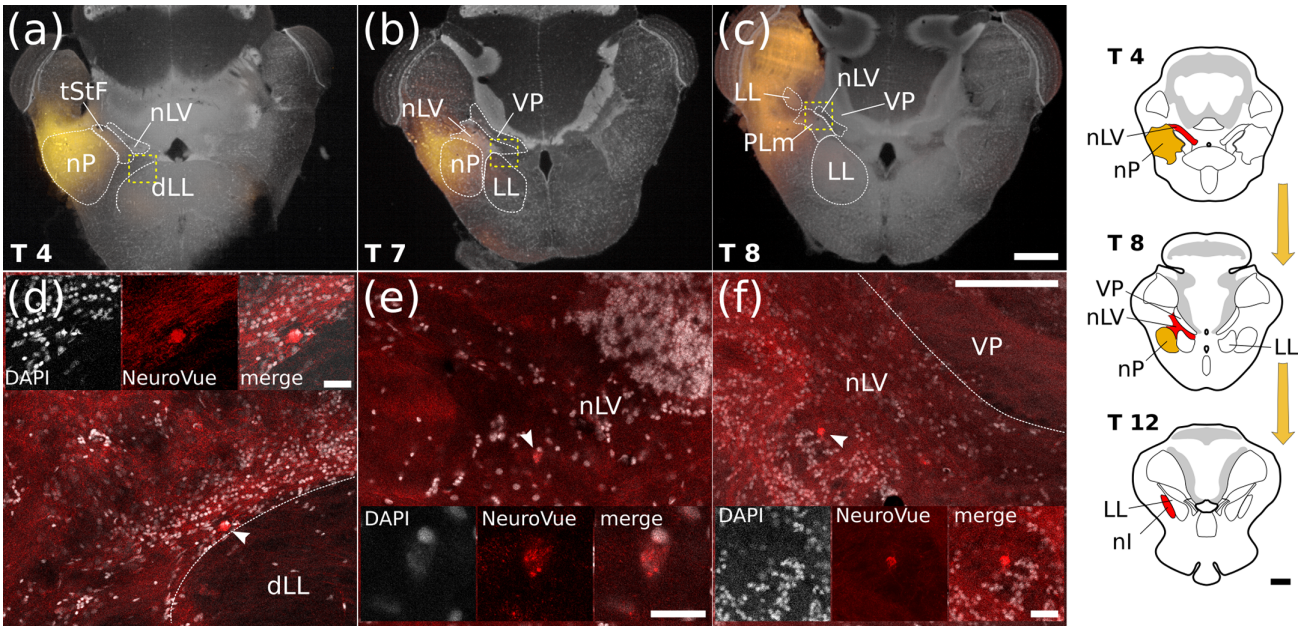

FIGURE 9 Photomicrographs and reconstructions of carbocyanine-based dye (DiI and NeuroVue) applications onto the posterior nP (a–f). (a–c) Dye applications (NeuroVue) at more posterior levels (T4) allowed the identification of cells located closer to the targeted area (d) and in proximity to the nLV and the putative SG/V (e,f). The panels on the upper right show the localization of dye application (orange). The arrows indicate the location of the application sites and the direction of dye transport. The areas in which labeled cells were found are shown in red. Scale bars: 500 μm (diagram), 100 μm (a–f), 50 μm (details of double positive cells in d–f). Since image acquisition was set to detect the minimum labeling intensity in the specimen and kept constant across all section, the dye application sites appear overexposed [Color figure can be viewed at wileyonlinelibrary.com]

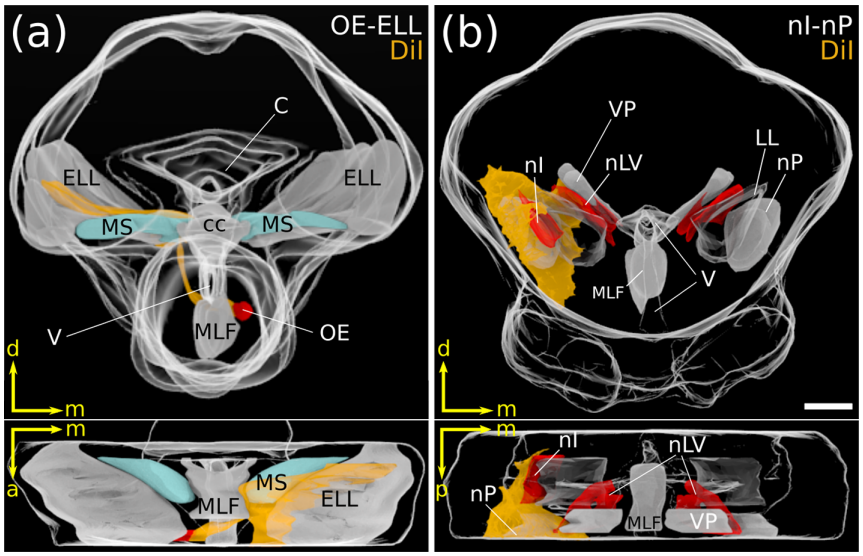

FIGURE 10 Reconstruction of DiI-stained neuronal tracts reconstructed in 3D from consecutive 50 μm serial sections obtained from two representative tracing experiments (front view: Top panels, top view: Bottom panels). In the ELL (a) and nP (b), DiI staining is shown in orange while putative sources of traced axons are indicated in red. Scale bar: 500 μm. Axes directions are indicated by the yellow arrows (d: dorsal, m: medial, a: anterior, p: posterior) [Color figure can be viewed at wileyonlinelibrary.com]

the neurons labeled in our tracing experiments to the nLV area, designated according to published anatomical references (Maler et al., 1991). In addition, we cannot exclude that in our tracing experiments targeting the nP we have retrogradely labeled fibers of passage belonging to any of these circuits, and therefore not projecting to nP. Future tracing studies will be required to further subdivide the isthmic nuclei in the light of these comparative observations, in order to precisely delineate their boundaries.

4.3.2 | Tectal cholinergic neurons

As in most vertebrates, the TeO plays a significant role in the integration of visual and other sensory inputs in the teleost mesencephalon (Bastian, 1982; Heiligenberg & Rose, 1987; Perez-Perez et al., 2003). It is involved in the generation of the orienting response and saccadic eye movements (Herrero et al., 1998; Luque et al., 2005), and the multisensory processing leading to selective object detection (Dunn

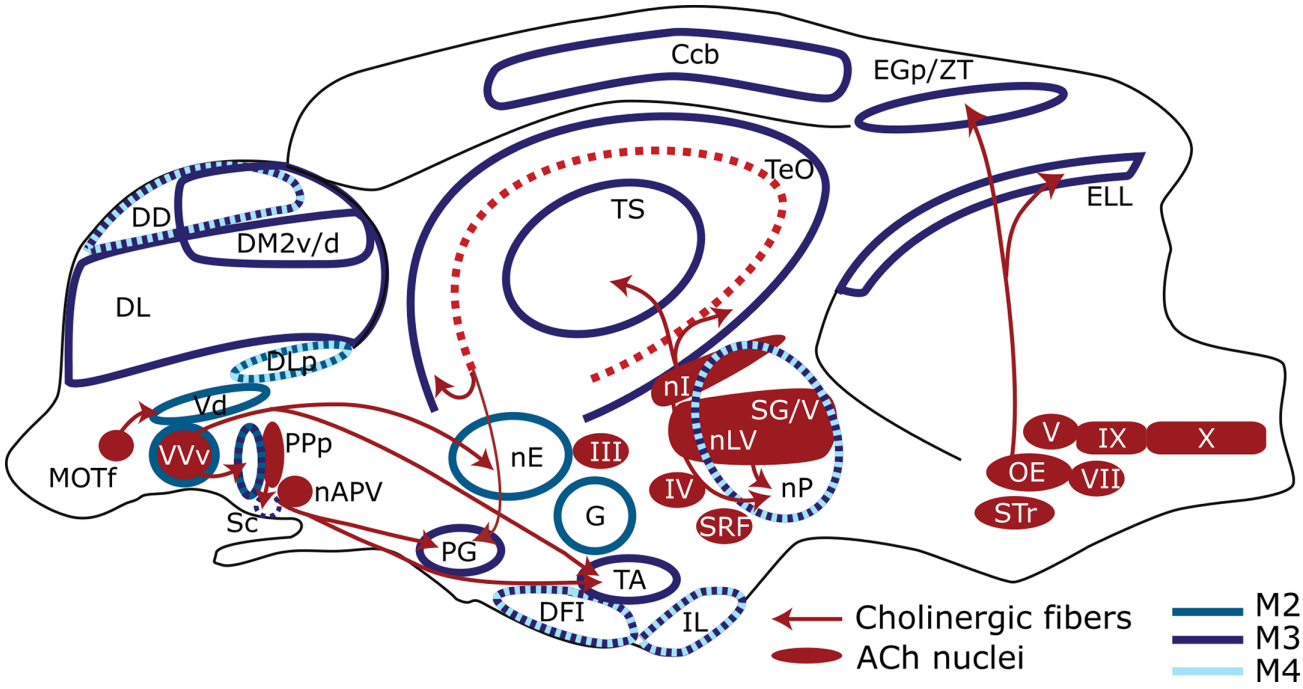

FIGURE 11 Sagittal brain representation summarizing the nonmotor elements of the cholinergic system in *Apteronotus leptorhynchus* brain. The nonmotor ChAT-containing nuclei that we found in this study are shown in red. Muscarinic receptor mRNA-containing nuclei are shown in different shades of blue (Toscano-Márquez, Dunn, & Krahe, 2013). Dark blue: muscarinic receptor 3 (M3); blue: muscarinic receptor 2 (M2); light blue: muscarinic receptor 4 (M4). Red arrows show the putative connections from the cholinergic nuclei to the muscarinic receptor-containing nuclei inferred from previous publications (Ahrens & Wullimann, 2002; Asadollahi et al., 2010; Giassi, Ellis, & Maler, 2012; Sas & Maler, 1987). The dashed vertical lines correspond to the figure panels indicated at the top. Ccb, corpus cerebelli; DD, dorsodorsal telencephalon; DFI, lateral subdivision of the diffuse nucleus; DL, dorsolateral telencephalon; DM2v/d, dorsomedial division of the telencephalon; EGp, eminentia granularis pars posterior; EO, efferent octavolateral n.; IL, inferior lobe; MOTf, medial olfactory terminal field; nAPV, nucleus anterior periventricularis; NE, n. electrosensorius; nl, n. isthmi; nLV, n. lateralis valvulae; nP, nucleus praeeminentialis; PG, preglomerular n.; PPa, anterior preoptic n.; PPp, posterior preoptic n.; TA, nucleus tuberis anterior; TeO, optic tectum; TS, torus semicircularis; Vd, dorsoventral telencephalon; Vvv, ventro-ventral telencephalon [Color figure can be viewed at wileyonlinelibrary.com]

et al., 2016; Knudsen, 2011). The TeO of *A. leptorhynchus* contains a large population of small cholinergic neurons with somata in the inner layer of the SPV (Figures 2(a_1) and 11; Sas & Maler, 1986b). Similar tectal ChAT-positive cells have been described in other teleosts (Clemente et al., 2004; López et al., 2013; Mueller et al., 2004; Pérez et al., 2000). These cholinergic neurons extend their dendrites and axons throughout several tectal layers, innervating cells in the outer layer of the stratum opticum and, to a lesser extent, cells in deeper layers of the TeO (Morona et al., 2013). In addition to these intrinsic cholinergic neurons, injections in the preglomerular nucleus (PG) of *A. leptorhynchus* revealed the presence of extrinsic efferents, retrogradely labeled in the SPV (Giassi, Duarte, et al., 2012). The morphology of these cells is similar to that of neurons immunolabeled with ChAT antibodies in two holostean fish species (Morona et al., 2013). Thus, although in other teleosts cholinergic SPV neurons have only been found to form intrinsic circuitry within TeO, our results together with those of Giassi, Duarte, et al. (2012) suggest that they also send cholinergic projections to PG, which we previously found to express muscarinic receptor mRNA densely (Figure 11; Toscano-Márquez, Dunn, & Krahe, 2013).

SPV (Heiligenberg & Rose, 1987) and PG (Wallach et al., 2018) neurons are known to respond strongly to electrosensory and visual object motion. Direct studies of the role of ACh in modulation of tectal and PG responses to visual and electrosensory motion stimuli will be required for a deeper understanding of how this transmitter regulates the encoding of motion stimuli (see also Bastian, 1982).

In our previous study, we found expression of mAChR2 and mAChR3 mRNA transcripts in both superficial (where intrinsic neurons are prominent) and deep layers (where extrinsic projection neurons reside) of the TeO (Figure 11; Toscano-Márquez, Dunn, & Krahe, 2013). Thus, intrinsic and extrinsic (nI) cholinergic innervation may be modulating both visual and electrosensory responses in tectum via M2 and M3 receptors.

4.4 | Cholinergic inputs to electrosensory areas

4.4.1 | Cholinergic input to nP: Isthmic efferent neurons

Our tracer injections in the nP resulted in retrograde labeling of several nI neurons (Figure 8(f)) as well as a great number of axons and several cell bodies stained dorsolateral to the LL, just medial to nP,

corresponding to the nLV and/or the SG/V areas (Figures 6(d–f) and 9 (e,f)), demonstrating a hitherto unknown input to the nP. Since the nP is tightly interconnected with the first central processing station of the electrosensory system, the ELL (Bastian et al., 2004; Maler et al., 1982; Sas & Maler, 1983), this cholinergic input could be acting indirectly on ELL as part of a previously hypothesized sensory searchlight mechanism (Bastian, 1999) and enhance the responses to object motion (Clarke & Maler, 2017).

Further physiological experiments will be critical to understanding the role of this cholinergic pathway on electrosensory processing. Injection of muscarinic agonists and antagonists into nP while recording from ELL pyramidal neurons would help elucidate the possible role of this modulatory input on the detection and processing of electrolocation stimuli.

4.4.2 | Cholinergic input to the ELL: The OE nucleus

Muscarinic ACh receptors are also present in the ELL of *A. leptorhynchus* (Figure 11; Phan & Maler, 1983; Toscano-Márquez, Dunn, & Krahe, 2013). Previous work suggested that the corresponding cholinergic input might arise from vertical fibers emanating from eurydendroid cells of the cerebellum (Maler et al., 1981). Even though some studies have found evidence for ChAT-positive cells in cerebellum in fish (Anadón et al., 2000) and mammals (Delacalle et al., 1993; Ikeda et al., 1991), our study is in agreement with most other work on teleosts and amphibians (see Morona et al., 2013, for a review) that showed the cerebellum to be devoid of cholinergic cells (Figure 5(b)). The cholinergic innervation in these cases has been suspected to derive from the reticular nucleus and the octavolateral area (Morona et al., 2013). The presence of cholinergic cells in both areas has been consistently reported as a conserved feature in fish and other vertebrates (Clemente et al., 2004; López et al., 2013; Morona et al., 2013). In this study, we found a small population of ChAT-positive cells in the RF close to the MLF as well as a prominent paramedian population on either side of the MLF in the octavolateral area corresponding to the OE in other fish (Figures 5(a) and 6(a); Clemente et al., 2004; Tomchik & Lu, 2006).

The injections of dextran-conjugated tetramethylrhodamine into the molecular layer of the ELL terminated in the contralateral OE area (Figure 6(c,d)). As no projections from ELL toward OE have ever been found (Krahe & Maler, 2014), we hypothesize that the fibers observed here provide cholinergic input from OE to ELL. This is confirmed by our DiI tracing experiments, showing retrogradely labeled cell bodies in the OE (Figure 7(e)). Projections from OE to EGp have already been described (Sas & Maler, 1987), which raises the possibility of the connections to ELL being collaterals of the projection to EGp. This latter connection is further supported by the presence of M3 receptors in eurydendroid cells in EGp (Figure 11; Toscano-Márquez, Dunn, & Krahe, 2013). Therefore, we hypothesize that OE is involved in direct cholinergic modulation of ELL processing as well as in indirect effects via modulation of cerebellar feedback to ELL.

Besides the well characterized role of the OE in the modulation of sensory organ activity (Katz et al., 2011; Köppl, 2011), to our knowledge, this may constitute the first example of OE modulation acting on a central nucleus. Further anatomical and physiological characterization of this cholinergic nucleus is required to confirm this hypothesis and further understand the functional and evolutionary implications of this finding. An additional interesting difference to previously described OE action is that the cholinergic effects in ELL are mediated by muscarinic ACh receptors and not by nicotinic receptors as in the other octavolateral systems (Katz et al., 2011; Köppl, 2011).

5 | CONCLUDING REMARKS

Overall, the spatial distribution of cholinergic neurons in the brain of the brown ghost knifefish, *A. leptorhynchus*, agrees with earlier descriptions in other teleosts and tetrapods. Connections between previously described muscarinic receptor-containing nuclei and cholinergic nuclei have been characterized in other studies in electric fish (Berman & Maler, 1999; Giassi, Ellis, & Maler, 2012; Sas & Maler, 1987) or can be inferred from previous cholinergic pathways in other teleosts based on homology (Figure 11; Ahrens & Wullimann, 2002; Asadollahi et al., 2010). In addition, the present study describes a new cholinergic input from the isthmic region (nI, nLV, and/or SG/V) to nP and from OE to ELL. These results suggest hitherto unrecognized additional levels of multisensory integration and control of electrosensory processing (Figure 11). Further targeted physiological experiments and connectivity analyses are required to explore the role of these pathways in behaving fish and to determine if these mechanisms evolved uniquely in gymnotiform weakly electric fishes or whether they are a general feature of the control of sensory information processing.

ACKNOWLEDGMENTS

Thanks to Anh-Tuan Trinh for his help with SeeDB processing of the retrogradely labeled brain sections, and to William Ellis, Sofia Ibarraran, and Ina Seuffert for technical assistance. Martin Cuddy helped with the partial cloning of aptChAT. The authors are grateful to Ehab Abouheif and François Fagotto for access to their lab equipment. This work was supported by Natural Sciences and Engineering Research Council of Canada (NSERC); Grant numbers: 2009-293306 and 2014-05364 (to R. K.); Grant sponsor: Le Fonds Quebecois de la Recherche sur la Nature et les Technologies (FQRNT); Grant number: FQRNT 2012 PR-145726 (to R. K.); Grant sponsor: Canada Foundation for Innovation; Grant number: 9604 (to R. K.); Grant sponsor: Canadian Institutes of Health Research (CIHR); Grant number: 6027 (to L. M.); Grant Sponsor NSERC; Grant number NSERC 04336 (to L. M.); Grant sponsor: Merit Scholarship for Foreign Students from FQRNT (to B. T. M.); Grant sponsor: Deutsche Forschungsgemeinschaft, NeuroCure Cluster of Excellence; Grant number: EXC257/2 (to R. K.).

CONFLICT OF INTEREST

The authors declare that the research was conducted in the absence of any conflict of interest.

AUTHOR CONTRIBUTIONS

Study concept and design: **Brenda Toscano-Márquez** and **Rüdiger Krahe**. Acquisition of data: **Brenda Toscano-Márquez**, **Livio Oboti**, and **Erik Harvey-Girard**. Analysis and interpretation of data: **Brenda Toscano-Márquez**, **Livio Oboti**, **Erik Harvey-Girard**, **Rüdiger Krahe**, and **Leonard Maler**. Drafting of the manuscript: **Brenda Toscano-Márquez** and **Rüdiger Krahe**. Critical revision of the manuscript for important intellectual content: **Erik Harvey-Girard**, **Leonard Maler**, and **Livio Oboti**

PEER REVIEW

The peer review history for this article is available at https://publons.com/publon/10.1002/cne.25058.

DATA AVAILABILITY STATEMENT

The data supporting the findings of this study are available from the corresponding author (L. O.) upon request.

ORCID

Livio Oboti https://orcid.org/0000-0001-7197-568X
Rüdiger Krahe https://orcid.org/0000-0003-1669-6121

REFERENCES

Adrio, F., Anadón, R., & Rodríguez-Moldes, I. (2000). Distribution of choline acetyltransferase (ChAT) immunoreactivity in the central nervous system of a chondrostean, the siberian sturgeon *Acipenser baeri*. *Journal of Comparative Neurology*, *426*, 602–621. https://doi.org/10.1002/1096-9861(20001030)426:4<602::AID-CNE8>3.0.CO;2-7.

Ahrens, K., & Wullimann, M. F. (2002). Hypothalamic inferior lobe and lateral torus connections in a percomorph teleost, the red cichlid *Hemichromis lifalili*. *Journal of Comparative Neurology*, *449*, 43–64. https://doi.org/10.1002/cne.10264.

Anadón, R., Molist, P., Rodríguez-Moldes, I., López, J. M., Quintela, I., Cerviño, M. C., Barja, P., & González, A. (2000). Distribution of choline acetyltransferase immunoreactivity in the brain of an elasmobranch, the lesser spotted dogfish *Scyliorhinus canicula*. *Journal of Comparative Neurology*, *420*, 139–170. https://doi.org/10.1002/(sici)1096-9861(20000501)420:2<139::aid-cne1>3.0.co;2-t.

Asadollahi, A., Mysore, S. P., & Knudsen, E. I. (2010). Stimulus-driven competition in a cholinergic midbrain nucleus. *Nature Neuroscience*, *13*, 889–895. https://doi.org/10.1038/nn.2573.

Asadollahi, A., Mysore, S. P., & Knudsen, E. I. (2011). Rules of competitive stimulus selection in a cholinergic isthmic nucleus of the owl midbrain. *Journal of Neuroscience*, *31*, 6088–6097. https://doi.org/10.1523/JNEUROSCI.0023-11.2011.

Baldo, B. A., Pratt, W. E., Will, M. J., Hanlon, E. C., Bakshi, V. P., & Cador, M. (2013). Principles of motivation revealed by the diverse functions of neuropharmacological and neuroanatomical substrates underlying feeding behavior. *Neuroscience Biobehavioral Reviews*, *37*, 1985–1998. https://doi.org/10.1016/j.neubiorev.2013.02.017.

Bastian, J. (1982). Vision and electroreception: Integration of sensory information in the optic tectum of the weakly electric fish *Apteronotus albifrons*. *Journal of Comparative Physiology*, *147*, 287–297. https://doi.org/10.1007/BF00609662.

Bastian, J. (1999). Plasticity of feedback inputs in the apteronotid electrosensory system. *Journal of Experimental Biology*, *202*, 1327–1337.

Bastian, J., Chacron, M. J., & Maler, L. (2004). Plastic and nonplastic pyramidal cells perform unique roles in a network capable of adaptive redundancy reduction. *Neuron*, *41*, 767–779. https://doi.org/10.1016/s0896-6273(04)00071-6.

Bell, C., & Maler, L. (2005). Central neuroanatomy of electrosensory systems in fish. In T. Bullock, C. Hopkins, A. Popper, & R. Fay (Eds.), *Electroreception*. Springer.

Berman, N., & Maler, L. (1999). Neural architecture of the electrosensory lateral line lobe: Adaptations for coincidence detection, a sensory searchlight and frequency-dependent adaptive filtering. *Journal of Experimental Biology*, *202*, 1243–1253.

Briscoe, S. D., & Ragsdale, C. W. (2019). Evolution of the chordate telencephalon. *Current Biology*, *29*, 647–662. https://doi.org/10.1016/j.cub.2019.05.026.

Casini, A., Vaccaro, R., Toni, M., & Cioni, C. (2018). Distribution of choline acetyltransferase (ChAT) immunoreactivity in the brain of the teleost *Cyprinus carpio*. *European Journal of Histochemistry*, *62*, 2932. https://doi.org/10.4081/ejh.2018.2932.

Castro, A., Becerra, M., Manso, M. J., & Anadón, R. (2006). Calretinin immunoreactivity in the brain of the zebrafish, *Danio rerio*: Distribution and comparison with some neuropeptides and neurotransmitter-synthesizing enzymes. II. Midbrain, hindbrain, and rostral spinal cord. *Journal of Comparative Neurology*, *494*, 792–814. https://doi.org/10.1002/cne.20843.

Chacron, M. J., Longtin, A., & Maler, L. (2011). Efficient computation via sparse coding in electrosensory neural networks. *Current Opinion in Neurobiology*, *21*, 752–760. https://doi.org/10.1016/j.conb.2011.05.016.

Chan, W., Singh, S., Keshav, T., Dewan, R., Eberly, C., Maurer, R., Nunez-Parra, A., & Araneda, R. (2017). Mice lacking M1 and M3 muscarinic acetylcholine receptors have impaired odor discrimination and learning. *Frontiers in Synaptic Neuroscience*, *9*, 4. https://dx.doi.org/10.3389/fnsyn.2017.00004.

Clarke, S. E., Longtin, A., & Maler, L. (2015). Contrast coding in the electrosensory system: Parallels with visual computation. *Nature Reviews in Neuroscience*, *16*, 733–744. https://doi.org/10.1038/nrn4037.

Clarke, S. E., & Maler, L. (2017). Feedback synthesizes neural codes for motion. *Current Biology*, *27*, 1356–1361. https://doi.org/10.1016/j.cub.2017.03.068.

Clemente, D., Arenzana, F. J., Sanchez-Gonzalez, R., Porteros, A., Aijon, J., & Arevalo, R. (2005). Comparative analysis of the distribution of choline acetyltransferase in the central nervous system of cyprinids. *Brain Research Bulletin*, *66*, 546–549. https://doi.org/10.1016/j.brainresbull.2005.02.017.

Clemente, D., Porteros, A., Weruaga, E., Alonso, J. R., Arenzana, F. J., Aijón, J., & Arévalo, R. (2004). Cholinergic elements in the zebrafish central nervous system: Histochemical and immunohistochemical analysis. *Journal of Comparative Neurology*, *474*, 75–107. https://doi.org/10.1002/cne.20111.

Contestabile, A., Migani, P., & Cristini, G. (1979). Choline acetyltransferase activity in the cerebellum and in centers of lateral line system of teleosts. *Brain Research Bulletin*, *4*, 859–861. https://doi.org/10.1016/0361-9230(79)90023-6.

Cronin, S. R., Khoury, A., Ferry, D. K., & Hampton, R. Y. (2000). Regulation of Hmg-Coa reductase degradation requires the P-type atpase Cod1p/Spf1p. *Journal of Cellular Biology*, *148*, 915–924. https://dx.doi.org/10.1083/jcb.148.5.915.

Danielson, P. D., Zottoli, S. J., Corrodi, J. G., Rhodes, K. J., & Mufson, E. J. (1988). Localization of choline acetyltransferase to somata of posterior lateral line efferents in the goldfish. *Brain Research*, *448*, 158–161. https://doi.org/10.1016/0006-8993(88)91112-2.

de Almeida, L., Idiart, M., Dean, O., Devore, S., Smith, D. M., & Linster, C. (2016). Internal cholinergic regulation of learning and recall in a model of olfactory processing. *Frontiers in Cellular Neuroscience*, *10*, 256. https://doi.org/10.3389/fncel.2016.00256.

Delacalle, S., Hersh, L. B., & Saper, C. B. (1993). Cholinergic innervation of the human cerebellum. *Journal of Comparative Neurology*, *328*, 364–376. https://doi.org/10.1002/cne.903280304.

Diamond, I. T., Fitzpatrick, D., & Conley, M. (1992). A projection from the parabigeminal nucleus to the pulvinar nucleus in galago. *Journal of Comparative Neurology*, *316*, 375–382. https://doi.org/10.1002/cne.903160308.

Dunlap, K. D., Chung, M., & Castellano, J. F. (2013). Influence of long-term social interaction on chirping behavior, steroid levels and neurogenesis in weakly electric fish. *Journal of Experimental Biology*, *216*, 2434–2441. https://doi.org/10.1242/jeb.082875.

Dunn, T. W., Gebhardt, C., Naumann, E. A., Riegler, C., Ahrens, M. B., Engert, F., & del Bene, F. (2016). Neural circuits underlying visually evoked escapes in larval zebrafish. *Neuron*, *89*, 613–628. https://doi.org/10.1016/j.neuron.2015.12.021.

Dutar, P., Bassant, M. H., Senut, M. C., & Lamour, Y. (1995). The septohippocampal pathway: Structure and function of a central cholinergic system. *Physiological Reviews*, *75*, 393–427. https://doi.org/10.1152/physrev.1995.75.2.393.

Ekström, P. (1987). Distribution of choline acetyltransferase-immunoreactive neurons in the brain of a cyprinid teleost (*Phoxinus phoxinus* L.). *Journal of Comparative Neurology*, *256*, 494–495. https://doi.org/10.1002/cne.902560403.

Ellis, L. D., Krahe, R., Bourque, C. W., Dunn, R. J., & Chacron, M. J. (2007). Muscarinic receptors control frequency tuning through the down-regulation of an A-type potassium current. *Journal of Neurophysiology*, *98*, 1526–1537. https://dx.doi.org/10.1152/jn.00564.2007.

Ericsson, J., Silberberg, G., Robertson, B., Wikstrom, M. A., & Grillner, S. (2011). Striatal cellular properties conserved from lampreys to mammals. *Journal of Physiology*, *589*, 2979–2992. https://doi.org/10.1113/jphysiol.2011.209643.

Felsenstein, J. (1989). PHYLIP-Phylogeny inference package. *Cladistics*, *5*, 164–166.

Fernandes, A. M., Larsch, J., Donovan, J. C., Helmbrecht, T. O., Mearns, D., Kölsch, Y., Dal Maschio, M., & Baier, H. (2019). Neuronal circuitry for stimulus selection in the visual system. *bioRxiv preprint*doi: https://doi.org/10.1101/598383.

Fournier, G. N., Semba, K., & Rasmusson, D. D. (2004). Modality- and region-specific acetylcholine release in the rat neocortex. *Neuroscience*, *126*, 257–262. https://doi.org/10.1016/j.neuroscience.2004.04.002.

Gallagher, S. P., & Northmore, D. P. M. (2006). Responses of the teleostean nucleus isthmi to looming objects and other moving stimuli. *Visual Neuroscience*, *23*, 209–219. https://doi.org/10.1017/s0952523806232061.

Ganz, J., Kaslin, J., Freudenreich, D., Machate, A., Geffarth, M., & Brand, M. (2012). Subdivisions of the adult zebrafish subpallium by molecular marker analysis. *Journal of Comparative Neurology*, *520*, 633–655. https://doi.org/10.1002/cne.22757.

Giassi, A. C. C., Duarte, T. T., Ellis, W., & Maler, L. (2012). Organization of the gymnotiform fish pallium in relation to learning and memory: II. Extrinsic connections. *Journal of Comparative Neurology*, *520*(3), 338–3368. https://doi.org/10.1002/cne.23109.

Giassi, A. C. C., Ellis, W., & Maler, L. (2012). Organization of the gymnotiform fish pallium in relation to learning and memory: III. Intrinsic connections. *Journal of Comparative Neurology*, *520*(3), 369–3394. https://doi.org/10.1002/cne.23108.

Giassi, A. C. C., Harvey-Girard, E., Valsamis, B., & Maler, L. (2012). Organization of the gymnotiform fish pallium in relation to learning and memory: I. Cytoarchitectonics and cellular morphology. *Journal of Comparative Neurology*, *520*(3), 314–3337. https://doi.org/10.1002/cne.23108.

González, A., Morona, R., Moreno, N., Bandín, S., & López, J. M. (2014). Identification of striatal and pallidal regions in the subpallium of anamniotes. *Brain Behavior and Evolution*, *83*, 93–103. https://doi.org/10.1159/000357754.

Govindasamy, L., Pedersen, B., Lian, W., Kukar, T., Gu, Y., Jin, S., Agbandje-McKenna, M., Wu, D., & McKenna, R. (2004). Structural insights and functional implications of choline acetyltransferase. *Journal of Structural Biology*, *148*, 226–235. https://doi.org/10.1016/j.jsb.2004.06.005.

Harvey-Girard, E., Giassi, A. C. C., Ellis, W., & Maler, L. (2012). Organization of the gymnotiform fish pallium in relation to learning and memory: IV. Expression of conserved transcription factors and implications for the evolution of dorsal telencephalon. *Journal of Comparative Neurology*, *520*(3), 395–3413. https://doi.org/10.1002/cne.23107.

Harvey-Girard, E., Giassi, A. C. C., Ellis, W., & Maler, L. (2013). Expression of the cannabinoid CB1 receptor in the gymnotiform fish brain and its implications for the organization of the teleost pallium. *Journal of Comparative Neurology*, *521*, 949–975. https://doi.org/10.1002/cne.23212.

Harvey-Girard, E., Tweedle, J., Ironstone, J., Cuddy, M., Ellis, W., & Maler, L. (2010). Long-term recognition memory of individual conspecifics is associated with telencephalic expression of Egr-1 in the electric fish *Apteronotus leptorhynchus*. *Journal of Comparative Neurology*, *518*, 2666–2692. https://doi.org/10.1002/cne.22358.

Hasegawa, K., & Ogawa, H. (2007). Effects of acetylcholine on coding of taste information in the primary gustatory cortex in rats. *Experimental Brain Research*, *179*, 97–109. https://doi.org/10.1007/s00221-006-0772-4.

Hasselmo, M. E. (2006). The role of acetylcholine in learning and memory. *Current Opinion in Neurobiology*, *16*, 710–715. https://dx.doi.org/10.1016/j.conb.2006.09.002.

Heiligenberg, W., Keller, C., Metzner, W., & Kawasaki, M. (1991). Structure and function of neurons in the complex of the nucleus electrosensorius of the gymnotiform fish *Eigenmannia*: Detection and processing of electric signals in social communication. *Journal of Comparative Physiology*, *169*, 151–164. https://doi.org/10.1007/BF00215862.

Heiligenberg, W., & Rose, G. J. (1987). The optic tectum of the gymnotiform electric fish, *Eigenmannia*: Labeling of physiologically identified cells. *Neuroscience*, *22*, 331–340. https://doi.org/10.1016/0306-4522(87)90224-7.

Heilingoetter, C. L., & Jensen, M. B. (2016). Histological methods for ex vivo axon tracing: A systematic review. *Neurological Research*, *38*, 561–569. https://doi.org/10.1080/01616412.2016.1153820.

Henriques, P. M., Rahman, N., Jackson, S. E., & Bianco, I. H. (2019). Nucleus isthmi is required to sustain target pursuit during visually guided prey-catching. *Current Biology*, *29*, 1771–1786. https://doi.org/10.1016/j.cub.2019.04.064.

Herrero, L., Rodriguez, F., Salas, C., & Torres, B. (1998). Tail and eye movements evoked by electrical microstimulation of the optic tectum in goldfish. *Experimental Brain Research*, *120*, 291–305. https://doi.org/10.1007/s002210050403.

Hofmann, V., & Chacron, M. J. (2019). Novel functions of feedback in electrosensory processing. *Frontiers in Integrative Neuroscience*, *13*, 52. https://dx.doi.org/10.3389/fnint.2019.00052.

Ichikawa, T., Ajiki, K., Matsuura, J., & Misawa, H. (1997). Localization of two cholinergic markers, choline acetyltransferase and vesicular acetylcholine transporter in the central nervous system of the rat: In situ hybridization histochemistry and immunohistochemistry. *Journal of Chemical Neuroanatomy*, *13*, 23–39. https://doi.org/10.1016/s0891-0618(97)00021-5.

Ikeda, M., Houtani, T., Ueyama, T., & Sugimoto, T. (1991). Choline-acetyltransferase immunoreactivity in the cat cerebellum. *Neuroscience*, *45*, 671–690. https://doi.org/10.1016/0306-4522(91)90280-2.

Imura, K., Yamamoto, N., Sawai, N., Yoshimoto, M., Yang, C. Y., Xue, H. G., & Ito, H. (2003). Topographical organization of an indirect telencephalo-cerebellar pathway through the nucleus paracommissuralis in a teleost, *Oreochromis niloticus*. *Brain Behavior and Evolution*, *61*, 70–90. https://doi.org/10.1159/000069353.

Ito, H., & Yoshimoto, M. (1990). Cytoarchitecture and fiber connections of the nucleus lateralis valvulae in the carp *Cyprinus carpio*. *Journal of Comparative Neurology*, *298*, 385–399. https://doi.org/10.1002/cne.902980402.

Jensen-Smith, H., Gray, B., Muirhead, K., Ohlsson-Wilhelm, B., & Fritzsch, B. (2007). Long-distance three-color neuronal tracing in fixed tissue using NeuroVue dyes. *Immunological Investigations*, *36*, 763–789. https://doi.org/10.1080/08820130701706711.

Jones, B. E. (2003). Arousal systems. *Frontiers in Bioscience*, *8*, S438–S451. https://doi.org/10.2741/1074.

Jun, J. J., Longtin, A., & Maler, L. (2016). Active sensing associated with spatial learning reveals memory-based attention in an electric fish. *Journal of Neurophysiology*, *115*, 2577–2592. https://doi.org/10.1152/jn.00979.2015.

Kasashima, S., Muroishi, Y., Futakuchi, H., Nakanishi, I., & Oda, Y. (1998). In situ mRNA hybridization study of the distribution of choline acetyltransferase in the human brain. *Brain Research*, *806*, 8–15. https://doi.org/10.1016/s0006-8993(98)00677-5.

Katz, E., Elgoyhen, A., & Fuchs, P. (2011). Cholinergic inhibition of hair cells. In D. K. Ryugo & R. R. Fay (Eds.), *Auditory and vestibular efferents*. Springer.

Ke, M., Fujimoto, S., & Imai, T. (2013). Optical Clearing of Fixed Brain Samples Using SeeDB. *Nature Neuroscience*, *16*, 1154–1161. https://doi.org/10.1002/0471142301.ns0222s66.

Kimura, F. (2000). Cholinergic modulation of cortical function: A hypothetical role in shifting the dynamics in cortical network. *Neuroscience Research*, *38*, 19–26. https://doi.org/10.1016/s0168-0102(00)00151-6.

Knudsen, E. I. (2011). Control from below: The role of a midbrain network in spatial attention. *European Journal of Neuroscience*, *33*, 1961–1972. https://doi.org/10.1111/j.1460-9568.2011.07696.x.

Köppl, C. (2011). Evolution of the octavolateral efferent system. In D. K. Ryugo & R. R. Fay (Eds.), *Auditory and vestibular efferents*. Springer.

Krahe, R., & Maler, L. (2014). Neural maps in the electrosensory system of weakly electric fish. *Current Opinion in Neurobiology*, *24*, 13–21. https://doi.org/10.1016/j.conb.2013.08.013.

Linke, R., Pabst, T., & Frotscher, M. (1995). Development of the hippocamposeptal projection in the rat. *Journal of Comparative Neurology*, *351*, 602–616. https://doi.org/10.1002/cne.903510409.

López, J. M., Perlado, J., Morona, R., Northcutt, R. G., & González, A. (2013). Neuroanatomical organization of the cholinergic system in the central nervous system of a basal actinopterygian fish, the Senegal bichir *Polypterus senegalus*. *Journal of Comparative Neurology*, *521*, 24–49. https://doi.org/10.1002/cne.23155.

Luque, M. A., Pérez-Pérez, M. P., Herrero, L., & Torres, B. (2005). Involvement of the optic tectum and mesencephalic reticular formation in the generation of saccadic eye movements in goldfish. *Brain Research Reviews*, *49*, 388–397. https://doi.org/10.1016/j.brainresrev.2004.10.002.

Maczko, K. A., Knudsen, P. F., & Knudsen, E. I. (2006). Auditory and visual space maps in the cholinergic nucleus isthmi pars parvocellularis of the barn owl. *Journal of Neuroscience*, *26*, 12799–12806. https://doi.org/10.1523/JNEUROSCI.3946-06.2006.

Maler, L., Collins, M., & Mathieson, W. B. (1981). The distribution of acetylcholinesterase and choline acetyl transferase in the cerebellum and posterior lateral line lobe of weakly electric fish (Gymnotidae). *Brain Research*, *226*, 320–325. https://doi.org/10.1016/0006-8993(81)91106-9.

Maler, L., Sas, E., Carr, C. E., & Matsubara, J. (1982). Efferent projections of the posterior lateral line lobe in gymnotiform fish. *Journal of Comparative Neurology*, *211*, 154–164. https://doi.org/10.1002/cne.902110205.

Maler, L., Sas, E., Johnston, S., & Ellis, W. (1991). An atlas of the brain of the electric fish *Apteronotus leptorhynchus*. *Journal of Chemical Neuroanatomy*, *4*, 1–38. https://doi.org/10.1016/0891-0618(91)90030-g.

Martinez-Gonzalez, C., Bolam, J. P., & Mena-Segovia, J. (2011). Topographical organization of the pedunculopontine nucleus. *Frontiers in Neuroanatomy*, *5*, 22. https://dx.doi.org/10.3389/fnana.2011.00022.

Meek, J., & Schellart, N. A. (1978). A Golgi study of goldfish optic tectum. *Journal of Comparative Neurology*, *182*, 89–122. https://doi.org/10.1002/cne.901820107.

Mooney, D. M., Zhang, L., Basile, C., Senatorov, V. V., Ngsee, J., Omar, A., & Hu, B. (2004). Distinct forms of cholinergic modulation in parallel thalamic sensory pathways. *PNAS*, *101*, 320–324. https://dx.doi.org/10.1073/pnas.0304445101.

Morona, R., López, J. M., Northcutt, R. G., & González, A. (2013). Comparative analysis of the organization of the cholinergic system in the brains of two holostean fishes, the Florida *Gar Lepisosteus platyrhincus* and the bowfin *Amia calva*. *Brain Behavior and Evolution*, *81*, 109–142. https://doi.org/10.1159/000347111.

Mueller, T., Vernier, P., & Wullimann, M. F. (2004). The adult central nervous cholinergic system of a neurogenetic model animal, the zebrafish *Danio rerio*. *Brain Research*, *1011*, 156–169. https://doi.org/10.1016/j.brainres.2004.02.073.

Mueller, T., Wullimann, M. F., & Guo, S. (2008). Early teleostean basal ganglia development visualized by Zebrafish Dlx2a, Lhx6, Lhx7, Tbr2 (eomesa), and GAD67 gene expression. *Journal of Comparative Neurology*, *507*, 1245–1257. https://doi.org/10.1002/cne.21604.

Nieuwenhuys, R. (2009). The forebrain of actinopterygians revisited. *Brain Behavior and Evolution*, *73*, 229–252. https://doi.org/10.1159/000225622.

Northmore, D. P. (1991). Visual responses of nucleus isthmi in a teleost fish *Lepomis macrochirus*. *Vision Research*, *31*, 525–535. https://doi.org/10.1016/0042-6989(91)90103-C.

Oboti, L., Russo, E., Tran, T., Durstewitz, D., & Corbin, J. (2018). Amygdala Corticofugal input shapes mitral cell responses in the accessory olfactory bulb. *eNeuro*, *5*, ENEURO.0175–ENEU18.2018. https://doi.org/10.1523/ENEURO.0175-18.2018.

Oda, Y. (1999). Choline acetyltransferase: The structure, distribution and pathologic changes in the central nervous system. *Pathology International*, *49*, 921–937. https://doi.org/10.1046/j.1440-1827.1999.00977.x.

Ohno, K., Tsujino, A., Brengman, J. M., Harper, C. M., Bajzer, Z., Udd, B., Beyring, R., Robb, S., Kirkham, F. J., & Engel, A. G. (2001). Choline acetyltransferase mutations cause myasthenic syndrome associated with episodic apnea in humans. *PNAS*, *98*, 2016–2022. https://doi.org/10.1073/pnas.98.4.2017.

Pérez, S. E., Yáñez, J., Marín, O., Anadón, R., González, A., & Rodríguez-Moldes, I. (2000). Distribution of choline acetyltransferase (ChAT) immunoreactivity in the brain of the adult trout and tract-tracing observations on the connections of the nuclei of the isthmus. *Journal Comparative Neurology*, *428*, 450–474. https://doi.org/10.1002/1096-9861(20001218)428:3%3C450::aid-cne5%3E3.0.co;2-t.

Perez-Perez, M. P., Luque, M. A., Herrero, L., Nunez-Abades, P. A., & Torres, B. (2003). Afferent connectivity to different functional zones of the optic tectum in goldfish. *Visual Neuroscience*, *20*, 397–410. https://doi.org/10.1017/S0952523803204053.

Phan, M., & Maler, L. (1983). Distribution of muscarinic receptors in the caudal cerebellum and electrosensory lateral line lobe of gymnotiform fish. *Neuroscience Letters*, *42*, 137–143. https://doi.org/10.1016/0304-3940(83)90396-8.

Picciotto, M. R., Higley, M. J., & Mineur, Y. S. (2012). Acetylcholine as a neuromodulator: Cholinergic signaling shapes nervous system function and behavior. *Neuron*, *76*, 116–129. https://dx.doi.org/10.1016/j.neuron.2012.08.036.

Salisbury, J. P., Sîrbulescu, R. F., Moran, B. M., Auclair, J. R., Zupanc, G. K. H., & Agar, J. N. (2015). The central nervous system transcriptome of the weakly electric brown ghost knifefish *Apteronotus leptorhynchus*: de novo assembly, annotation, and proteomic validation. *BMC Genomics*, *16*, 166. https://doi.org/10.1186/s12864-015-1354-2.

Sarter, M., Hasselmo, M. E., Bruno, J. P., & Givens, B. (2005). Unraveling the attentional functions of cortical cholinergic inputs: Interactions between signal-driven and cognitive modulation of signal detection. *Brain Research Reviews*, *48*, 98–111. https://doi.org/10.1016/j.brainresrev.2004.08.006.

Sas, E., & Maler, L. (1983). The nucleus praeeminentialis: A Golgi study of a feedback center in the electrosensory system of gymnotid fish. *Journal*

of Comparative Neurology, *221*, 127–144. https://doi.org/10.1002/cne.902210202.

Sas, E., & Maler, L. (1986a). Identification of a nucleus isthmi in the weakly electric fish *Apteronotus leptorhynchus* (Gymnotiformes). *Brain Behavior and Evolution*, *28*, 170–185. https://doi.org/10.1159/000118701.

Sas, E., & Maler, L. (1986b). The optic tectum of gymnotiform teleosts *Eigenmannia virescens* and *Apteronotus leptorhynchus*: A Golgi study. *Neuroscience*, *18*, 215–246. https://doi.org/10.1016/0306-4522(86)90190-9.

Sas, E., & Maler, L. (1987). The organization of afferent input to the caudal lobe of the cerebellum of the gymnotid fish *Apteronotus leptorhynchus*. *Anatomy and Embryology*, *177*, 55–79. https://doi.org/10.1007/BF00325290.

Sas, E., Maler, L., & Weld, M. (1993). Connections of the olfactory bulb in the gymnotiform fish, *Apteronotus leptorhynchus*. *Journal of Comparative Neurology*, *335*, 486–507. https://doi.org/10.1002/cne.903350403.

Sato, H., Hata, Y., Masui, H., & Tsumoto, T. (1987). A functional-role of cholinergic innervation to neurons in the cat visual-cortex. *Journal of Neurophysiology*, *58*, 765–780. https://doi.org/10.1152/jn.1987.58.4.765.

Schmidt, J. T. (1995). The modulatory cholinergic system in goldfish tectum may be necessary for retinotopic sharpening. *Visual Neuroscience*, *12*, 1093–1103. https://doi.org/10.1017/s095252380000674x.

Sillito, A. M., & Kemp, J. A. (1983). Cholinergic modulation of the functional-organization of the cat visual-cortex. *Brain Research*, *289*, 143–155. https://doi.org/10.1016/0006-8993(83)90015-X.

Sillito, A. M., Kemp, J. A., & Berardi, N. (1983). The cholinergic influence on the function of the cat dorsal lateral geniculate-nucleus (DLGN). *Brain Research*, *280*, 299–307. https://doi.org/10.1016/0006-8993(83)90059-8.

Silva, A. C., Perrone, R., Zubizarreta, L., Batista, G., & Stoddard, P. K. (2013). Neuromodulation of the agonistic behavior in two species of weakly electric fish that display different types of aggression. *Journal of Experimental Biology*, *216*, 2412–2420. https://doi.org/10.1242/jeb.082180.

Smith, R. S., Hu, R., DeSouza, A., Eberly, C. L., Krahe, K., Chan, W., & Araneda, R. C. (2015). Differential muscarinic modulation in the olfactory bulb. *Journal of Neuroscience*, *35*, 10773–10785. https://doi.org/10.1523/JNEUROSCI.0099-15.2015.

Stephenson-Jones, M., Ericsson, J., Robertson, B., & Grillner, S. (2012). Evolution of the basal ganglia: Dual-output pathways conserved throughout vertebrate phylogeny. *Journal of Comparative Neurology*, *520*, 2957–2973. https://doi.org/10.1002/cne.23087.

Tomchik, S. M., & Lu, Z. (2006). Auditory physiology and anatomy of octavolateral efferent neurons in a teleost fish. *Journal of Comparative Physiology*, *192*, 51–67. https://doi.org/10.1007/s00359-005-0050-0.

Toscano-Márquez, B., Dunn, R. J., & Krahe, R. (2013). Distribution of muscarinic acetylcholine receptor mRNA in the brain of the weakly electric fish *Apteronotus leptorhynchus*. *Journal of Comparative Neurology*, *521*, 1054–1072. https://doi.org/10.1002/cne.23218.

Toscano-Márquez, B., Krahe, R., & Chacron, M. J. (2013). Neuromodulation of early electrosensory processing in gymnotiform weakly electric fish. *Journal of Experimental Biology*, *216*, 2442–2450. https://doi.org/10.1242/jeb.082370.

Wallach, A., Harvey-Girard, E., Jun, J. J., Longtin, A., & Maler, L. (2018). A time-stamp mechanism may provide temporal information necessary for egocentric to allocentric spatial transformations. *eLife*, *7*, e36769. https://doi.org/10.7554/elife.36769.

Walz, H., Hupe, G. J., Benda, J., & Lewis, J. E. (2013). The neuroethology of electrocommunication: How signal background influences sensory encoding and behaviour in *Apteronotus leptorhynchus*. *Journal of Physiology Paris*, *107*, 13–25. https://doi.org/10.1016/j.jphysparis.2012.07.001.

Wang, S. R. (2003). The nucleus isthmi and dual modulation of the receptive field of tectal neurons in non-mammals. *Brain Research Reviews*, *41*, 13–25. https://doi.org/10.1016/S0165-0173(02)00217-5.

Wang, Y., Luksch, H., Brecha, N. C., & Karten, H. J. (2006). Columnar projections from the cholinergic nucleus isthmi to the optic tectum in chicks (*Gallus gallus*): A possible substrate for synchronizing tectal channels. *Journal of Comparative Neurology*, *494*, 7–35. https://doi.org/10.1002/cne.20821.

Wong, C. J. H. (1997). Connections of the basal forebrain of the weakly electric fish, *Eigenmannia virescens*. *Journal of Comparative Neurology*, *389*, 49–64. https://doi.org/10.1002/(SICI)1096-9861(19971208)389:1<49::AID-CNE4>3.0.CO;2-E.

Woolf, N. J., & Butcher, L. L. (2011). Cholinergic systems mediate action from movement to higher consciousness. *Behavioral Brain Research*, *221*, 488–498. https://doi.org/10.1016/j.bbr.2009.12.046.

Wullimann, M. F., & Mueller, T. (2004). Teleostean and mammalian forebrains contrasted: Evidence from genes to behavior. *Journal of Comparative Neurology*, *475*, 143–162. https://doi.org/10.1002/cne.20183.

Wullimann, M. F., Rupp, B., & Reichert, H. (1996). The brain of the zebrafish *Danio rerio*: A neuroanatomical atlas. In *Neuroanatomy of the Zebrafish brain*. Birkhäuser Verlag.

Xue, H. G., Yamamoto, N., Yoshimoto, M., Yang, C. Y., & Ito, H. (2001). Fiber connections of the nucleus isthmi in the carp (*Cyprinus carpio*) and tilapia (*Oreochromis niloticus*). *Brain Behavior and Evolution*, *58*, 185–204. https://doi.org/10.1159/000057563.

Xue, H. G., Yang, C. Y., Yamamoto, N., Ito, H., & Ozawa, H. (2005). An indirect trigeminocerebellar pathway through the nucleus lateralis valvulae in a perciform teleost, *Oreochromis niloticus*. *Neuroscience Letters*, *390*, 104–108. https://doi.org/10.1016/j.neulet.2005.08.007.

Yáñez, J., Souto, Y., Piñeiro, L., Folgueira, M., & Anadón, R. (2017). Gustatory and general visceral centers and their connections in the brain of adult zebrafish: A carbocyanine dye tract-tracing study. *Journal of Comparative Neurology*, *525*, 333–362. https://doi.org/10.1002/cne.24068.

Yang, C. Y., Yoshimoto, M., Xue, H. G., Yamamoto, N., Imura, K., Sawai, N., Ishikawa, Y., & Ito, H. (2004). Fiber connections of the lateral valvular nucleus in a percomorph teleost, tilapia (*Oreochromis niloticus*). *Journal of Comparative Neurology*, *474*, 209–226. https://doi.org/10.1002/cne.20150.

Yasuyama, K., & Salvaterra, P. M. (1999). Localization of choline acetyltransferase-expressing neurons in *Drosophila* nervous system. *Microscopy Research and Technique*, *45*, 65–79. https://doi.org/10.1002/(sici)1097-0029(19990415)45:2<65::aid-jemt2>3.0.co;2-0.

Yoshida, K., Rutishauser, U., Crandall, J. E., & Schwarting, G. A. (1999). Polysialic acid facilitates migration of luteinizing hormone-releasing hormone neurons on vomeronasal axons. *Journal of Neuroscience*, *19*, 794–801. https://doi.org/10.1523/jneurosci.19-02-00794.1999.

Zottoli, S. J., Rhodes, K. J., Corrodi, J. G., & Mufson, E. J. (1988). Putative cholinergic projections from the nucleus isthmi and the nucleus reticularis mesencephali to the optic tectum in the goldfish (*Carassius auratus*). *Journal of Comparative Neurology*, *273*, 385–398. https://doi.org/10.1002/cne.902730309.

SUPPORTING INFORMATION

Additional supporting information may be found online in the Supporting Information section at the end of this article.

How to cite this article: Toscano-Márquez B, Oboti L, Harvey-Girard E, Maler L, Krahe R. Distribution of the cholinergic nuclei in the brain of the weakly electric fish, *Apteronotus leptorhynchus*: Implications for sensory processing. *J Comp Neurol*. 2020;1–20. https://doi.org/10.1002/cne.25058